Numerical Simulation of Ground-Water Flow Through Glacial Deposits and Crystalline Bedrock in the Mirror Lake Area, Grafton County, New Hampshire

U.S. GEOLOGICAL SURVEY PROFESSIONAL PAPER 1572

Numerical Simulation of Ground-Water Flow Through Glacial Deposits and Crystalline Bedrock in the Mirror Lake Area, Grafton County, New Hampshire

By CLAIRE R. TIEDEMAN, DANIEL J. GOODE, *and* PAUL A. HSIEH

U.S. GEOLOGICAL SURVEY PROFESSIONAL PAPER 1572

1997

U.S. DEPARTMENT OF THE INTERIOR

BRUCE BABBITT, Secretary

U.S. GEOLOGICAL SURVEY

Gordon P. Eaton, Director

Library of Congress Cataloging-in-Publications Data

Tiedeman, Claire R.

Numerical simulation of ground-water flow through glacial deposits and crystalline bedrock in the Mirror Lake area, Grafton County, New Hampshire / by Claire R. Tiedeman, Daniel J. Goode, and Paul A. Hsieh.

p. cm -- (U.S. Geological Survey professional paper ; 1572)
Includes bibliographical references.
Supt. of Docs. no.: I 19.16: 1572
1. Groundwater flow--New Hampshire--Mirror Lake (Grafton County)
I. Goode, Daniel J. II. Hsieh, P.A. (Paul A.) III. Title. IV. Series.
GB1197.7.T54 1997
551.49'09742'3--dc21

97-873
CIP

ISBN 0-607-86639-X

For sale by U.S. Geological Survey
Box 25286
Denver, CO 80225-0286

CONTENTS

FIGURES

TABLES

CONVERSION FACTORS AND VERTICAL DATUM

Multiply	By	To obtain
centimeter (cm)	0.394	inch
centimeter per year (cm/year)	0.394	inch per year
cubic meter per year (m^3/year)	35.320	cubic foot per year
kilometer (km)	0.622	mile
meter (m)	3.281	foot
meter per second (m/s)	3.281	foot per second
square kilometer (km^2)	0.387	square mile
square meter (m^2)	10.765	square foot

Temperature, given in degrees Celsius (°C), can be converted to degrees Fahrenheit (°F) by the following equation:

$$°F = 9/5\ (°C) + 32$$

Sea level: In this report, "sea level" refers to the National Geodetic Vertical Datum of 1929—a geodetic datum derived from a general adjustment of the first-order level nets of both the United States and Canada, formerly called Sea Level Datum of 1929.

NUMERICAL SIMULATION OF GROUND-WATER FLOW THROUGH GLACIAL DEPOSITS AND CRYSTALLINE BEDROCK IN THE MIRROR LAKE AREA, GRAFTON COUNTY, NEW HAMPSHIRE

By Claire R. Tiedeman, Daniel J. Goode, *and* Paul A. Hsieh

ABSTRACT

This report documents the development of a computer model to simulate steady-state (long-term average) flow of ground water in the vicinity of Mirror Lake, which lies at the eastern end of the Hubbard Brook valley in central New Hampshire. The 10-km^2 study area includes Mirror Lake, the three streams that flow into Mirror Lake, Leeman's Brook, Paradise Brook, and parts of Hubbard Brook and the Pemigewasset River. The topography of the area is characterized by steep hillsides and relatively flat valleys. Major hydrogeologic units include glacial deposits, composed of till containing pockets of sand and gravel, and fractured crystalline bedrock, composed of schist intruded by granite, pegmatite, and lamprophyre. Ground water occurs in both the glacial deposits and bedrock. Precipitation and snowmelt infiltrate to the water table on the hillsides, flow downslope through the saturated glacial deposits and fractured bedrock, and discharge to streams and to Mirror Lake.

The model domain includes the glacial deposits, the uppermost 150 m of bedrock, Mirror Lake, the layer of organic sediments on the lake bottom, and streams and rivers within the study area. A streamflow routing package was included in the model to simulate baseflow in streams and interaction between streams and ground water. Recharge from precipitation is assumed to be areally uniform, and riparian evapotranspiration along stream banks is assumed negligible. The spatial distribution of hydraulic conductivity is represented by dividing the model domain into several zones, each having uniform hydraulic properties. Local variations in recharge and hydraulic conductivities are ignored; therefore, the simulation results characterize the general ground-water system, not local details of ground-water movement.

The model was calibrated using a nonlinear regression method to match hydraulic heads measured in piezometers and wells, and baseflow in the three inlet streams to Mirror Lake. Model calibration indicates that recharge from precipitation to the water table is 26 to 28 cm/year. Hydraulic conductivities are 1.7×10^{-6} to 2.7×10^{-6} m/s for glacial deposits, about 3×10^{-7} m/s for bedrock beneath lower hillsides and valleys, and about 6×10^{-8} m/s for bedrock beneath upper hillsides and hilltops. Analysis of parameter uncertainty indicates that the above values are well constrained, at least within the context of regression analysis. In the regression, several attributes of the ground-water flow model are assumed perfectly known. The hydraulic conductivity for bedrock beneath upper hillsides and hilltops was determined from few data, and additional data are needed to further confirm this result. Model fit was not improved by introducing a 10-to-1 ratio of horizontal-to-vertical anisotropy in the hydraulic conductivity of the glacial deposits, or by varying hydraulic conductivity with depth in the modeled part (uppermost 150 m) of the bedrock.

The calibrated model was used to delineate the Mirror Lake ground-water basin, defined as the volume of subsurface through which ground water flows from the water table to Mirror Lake or its inlet streams. Results indicate that Mirror Lake and its inlet streams drain an area of ground-water recharge that is about 1.5 times the area of the surface-water basin. The ground-water basin extends far up the hillside on the northwestern part of the study area. Ground water from this area flows at depth under Norris Brook to discharge into Mirror Lake or its inlet streams. As a result, the Mirror Lake ground-water basin extends beneath the adjacent ground-water basin that drains into Norris Brook.

Model simulation indicates that approximately 300,000 m^3/year of precipitation recharges the Mirror Lake ground-water basin. About half the recharge enters the basin in areas where the simulated water table lies in glacial deposits; the other half enters the basin in areas where the simulated water table lies in bedrock. Flow from glacial deposits to bedrock occurs primarily beneath upper hillsides. Flow from bedrock to glacial deposits occurs primarily beneath lower hillsides and valleys. About 40 percent of the recharge (120,000 m^3/year) moves through the basin along flow paths that remain in glacial deposits; about 60 percent (180,000 m^3/year) moves along flow paths that pass through bedrock. Under steady state, total recharge to the basin equals total discharge from the basin. Of the total discharge, slightly more than half (170,000 m^3/year) flows into the three Mirror Lake inlet streams; slightly less than half (130,000 m^3/year) flows directly into Mirror Lake.

INTRODUCTION

BACKGROUND

The area in the vicinity of Mirror Lake, which lies at the eastern end of the Hubbard Brook valley in central New Hampshire, has long been the subject of ecologic and hydrologic investigations. In 1955, the Forest Service of the U.S. Department of Agriculture established the Hubbard Brook Experimental Forest, which includes nearly the entire Hubbard Brook valley, as a center for watershed-management research in the northeastern United States. During the 1960's, the Forest Service together with several academic institutions developed a long-term, multidisciplinary study at the Experimental Forest to investigate the structure and function of northern hardwood forest ecosystems. Since the late 1970's, the U.S. Geological Survey has been conducting ground-water studies in the Mirror Lake area. This report presents findings from a part of the U.S. Geological Survey studies.

The initial study by the U.S. Geological Survey intended to characterize the hydrologic system associated with Mirror Lake, with emphasis on the interaction between the lake and ground water. Beginning in 1979, Winter (1984) led a long-term effort to monitor lake evaporation, surface-water flow into and out of Mirror Lake, and ground-water conditions. The monitoring effort involved installation of a weather station, three stream gages, and a network of piezometers and bedrock wells. In addition, geophysical surveys and aquifer tests were carried out to determine the thickness and hydraulic conductivity of the glacial deposits. Results of this study established a basic understanding of the geohydrologic setting and the water budget of Mirror Lake.

In 1989, the U.S. Geological Survey began an additional study to investigate ground-water flow through fractured crystalline rocks that underlie the Mirror Lake area. This study seeks to develop hydrologic, geologic, geophysical, and geochemical methods to characterize ground-water flow and chemical transport in fractured rocks (Shapiro and Hsieh, 1991). Although the Mirror Lake area is not contaminated, the techniques and understanding developed in the study are transferable to other fractured rock sites that have been contaminated with chemical wastes. One component of the fractured-rock hydrology study is to develop a computer model to simulate the three-dimensional, steady-state flow of ground water through glacial deposits and crystalline bedrock in the Mirror Lake area. Results of this modeling study are presented in this report.

PURPOSE AND SCOPE

The purpose of the modeling study is to estimate, for the Mirror Lake area, (1) the rate of recharge from precipitation to the water table, (2) the hydraulic conductivity of glacial deposits and bedrock, (3) the three-dimensional extent of the Mirror Lake ground-water basin, and (4) the ground-water budget. The recharge rate is an average value over the entire study area. The hydraulic conductivities are effective values that characterize entire hydrogeologic units or large zones within units. The Mirror Lake ground-water basin refers to the volume of subsurface through which ground water flows from the water table to Mirror Lake, or to one of the streams that flow into Mirror Lake. The ground-water budget gives an accounting of recharge to the ground-water basin, discharge from the basin, and flow between hydrogeologic units in the basin.

The scope of the modeling study includes: (1) conceptualizing the ground-water system, (2) developing a computer model of the ground-water system, (3) calibrating the model to determine optimal parameters, and (4) simulating ground-water flow to determine the ground-water basin and ground-water budget. Conceptualization of the ground-water system is based on previous studies and hydrologic data that include: hydraulic heads measured in piezometers and wells, streamflow measured at stream gages, hydraulic properties determined from aquifer tests, and lithologic information obtained from field observations, well drilling, and geophysical measurements. Ground-water flow is simulated by the U.S. Geological Survey Modular Three-Dimensional Finite-Difference Ground-Water Flow Model (McDonald and Harbaugh, 1988), commonly known as MODFLOW. The model is calibrated using the computer program MODFLOWP (Hill, 1992), which employs nonlinear least-squares regression to determine optimal parameters. Included in the calibration process is an assessment of parameter uncertainty and goodness of model fit. The three-dimensional extent of the Mirror Lake ground-water basin is delineated by tracking ground-water flow paths with the computer program MODPATH (Pollock, 1994), a particle tracking post-processor package for MODFLOW. The ground-water budget is calculated using the computer program ZONEBUDGET (Harbaugh, 1990), which calculates subregional water budgets using simulation results from MODFLOW.

STUDY AREA

The study area is in central New Hampshire about 15 km north of the town of Plymouth (fig. 1). It occupies about 10 km^2, and includes Mirror Lake. The study area is bounded by the Pemigewasset River to the east, and Leeman's Brook to the north. The western boundary is formed by a small stream locally known as Paradise Brook, and a north-northeastward flowing segment of Hubbard Brook. The southern boundary is formed by the ridge south of Hubbard Brook. For the purpose of this report, the study area is referred to as the "Mirror Lake area."

Within the Mirror Lake area, the U.S. Geological Survey studies have focused on the Mirror Lake ground-water basin. At the outset, however, the extent of the ground-water basin was not well known. Therefore, the surface-water basin, an area of 0.85 km^2 outlined by the topographic divide surrounding Mirror Lake (fig. 2), was initially chosen as the area of focused investigation. As of 1994, most piezometers and bedrock wells in the Mirror Lake area were drilled within the surface-water basin (fig. 3). However, because it was expected that the surface-water basin might not entirely coincide with the ground-water basin, several piezometers and bedrock wells were drilled outside the surface-water basin.

PHYSICAL SETTING

The topography of the Mirror Lake area is characterized by steep hillsides and relatively flat valleys. The higher altitudes of the study area are dominated by ridges and bedrock knobs, which typically have a thin mantle of glacial deposits. Relatively flat kame terraces occur at several levels on the steep hillsides. At the lower altitudes, thicker glacial and alluvial deposits cover the slopes and valleys. Land-surface altitude ranges from 180 m above sea level at the Pemigewasset River to 700 m above sea level at the ridge top near the northwestern corner of the study area.

Within the Mirror Lake surface-water basin, land-surface altitude ranges from 213 m above sea level at the lake shore to 470 m above sea level at the

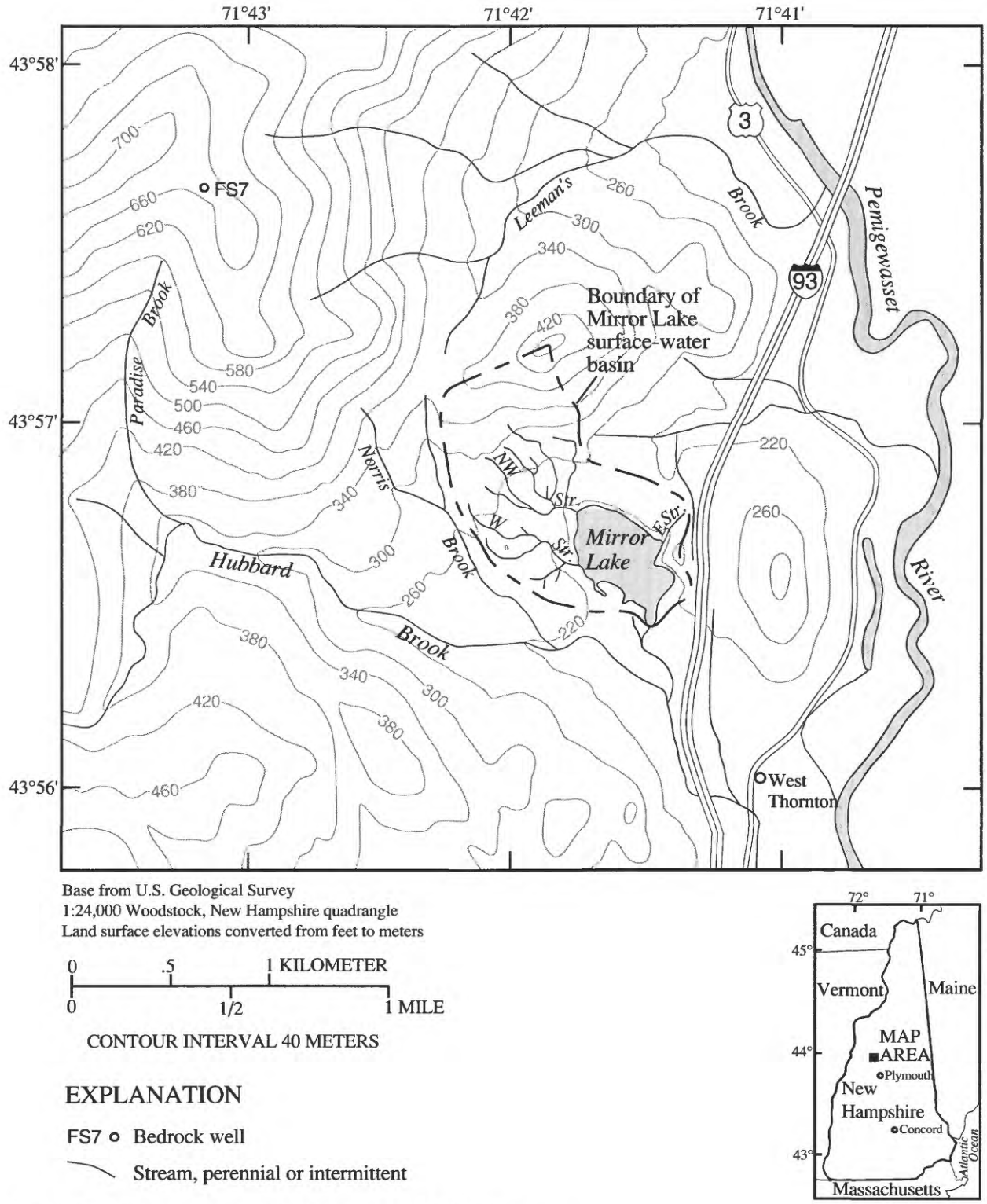

Figure 1. Location, extent, and topography of study area.

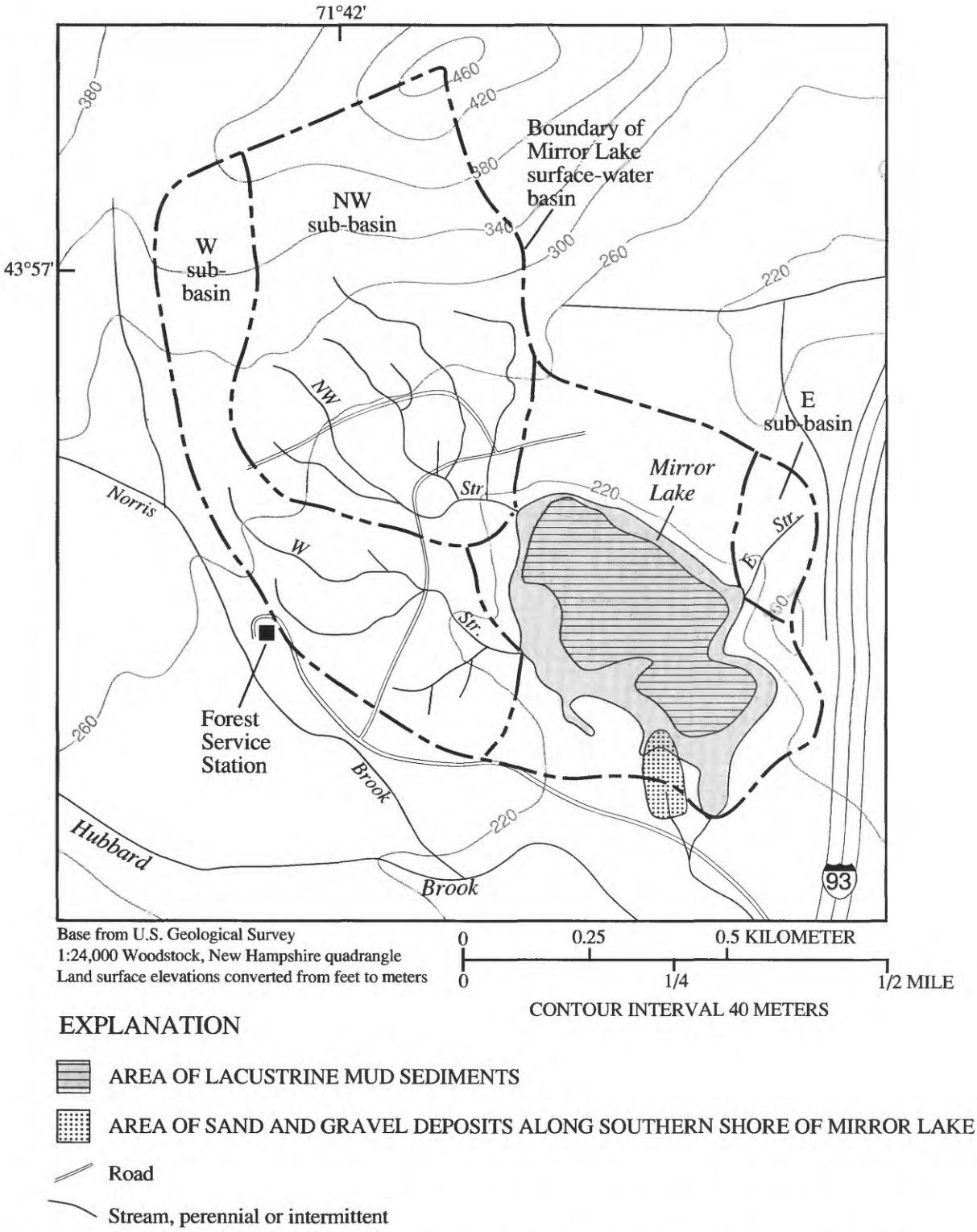

Figure 2. Mirror Lake surface-water basin; sub-basins W, NW, and E; area of lacustrine mud sediments; and area of sand and gravel deposits along southern shore of Mirror Lake.

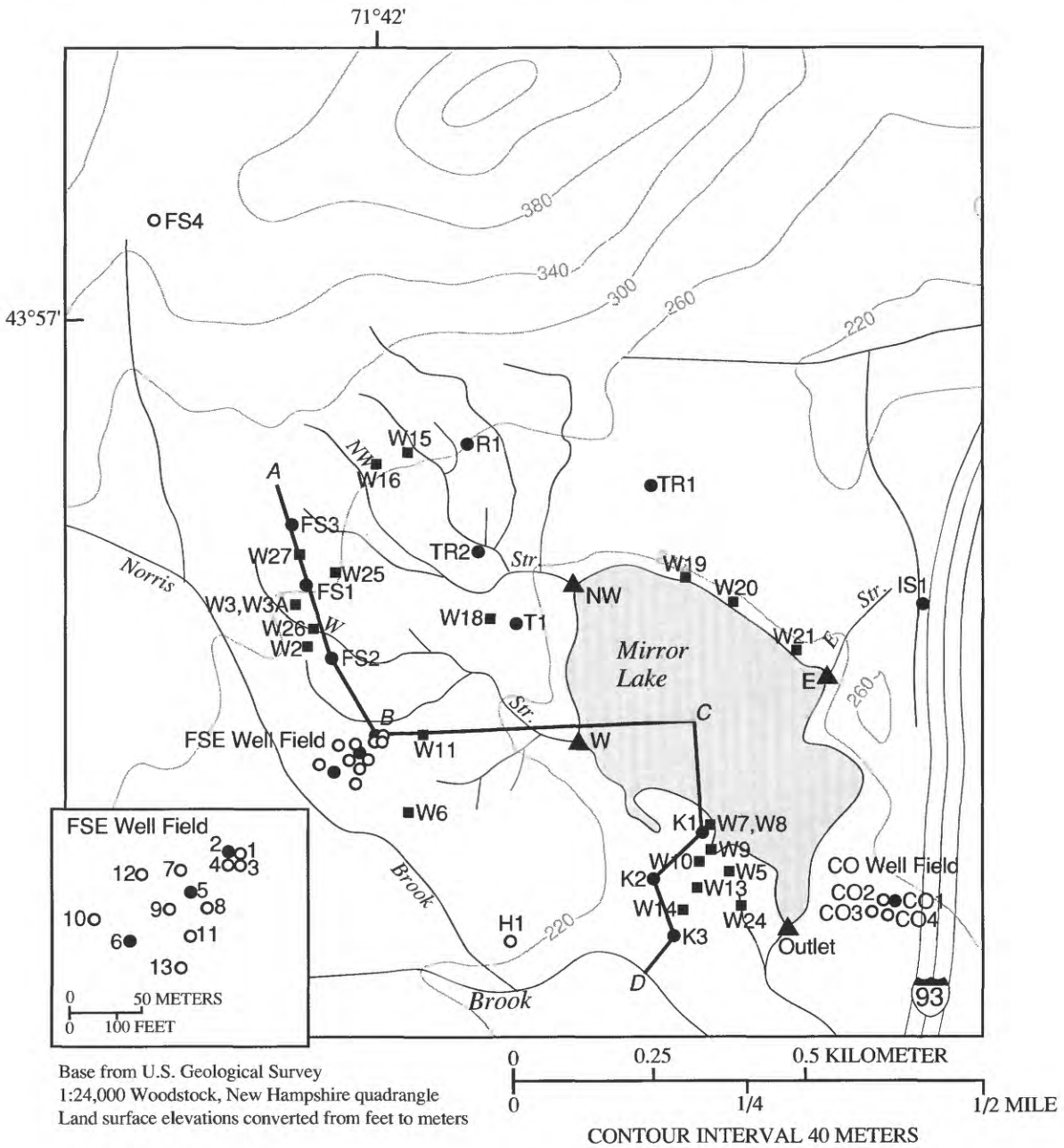

Base from U.S. Geological Survey
1:24,000 Woodstock, New Hampshire quadrangle
Land surface elevations converted from feet to meters

EXPLANATION

INSTRUMENTATION SITE AND IDENTIFIER

- E▲ Flume
- W2■ Piezometer
- T1● Bedrock well and Piezometer nest
- H1○ Bedrock well
- *A*—*D* LINE OF GEOLOGIC SECTION (See fig. 4)

Figure 3. Locations of flumes, piezometers, and bedrock wells as of 1994.

highest point of the drainage divide. The surface-water basin contains three sub-basins, which have been designated as W, NW, and E (fig. 2). Each sub-basin contains a perennial stream that flows into Mirror Lake. The streams are designated by the same names as their respective sub-basins. Streams W and NW have several tributaries, some of which are intermittent. Physiographic characteristics of the three sub-basins are described by Winter (1984).

Mirror Lake is a kettle lake occupying about 150,000 m^2 (Winter, 1985). The lake has a maximum depth of 11 m and an average depth of about 6 m (Winter, 1984). A small dam at the lake's outlet on the southern shore maintains a near-constant lake level. At the dam, the lake discharges into an outlet stream, which flows into Hubbard Brook.

The climate of the Mirror Lake area is classified as humid continental characterized by short, cool summers and long, cold winters (Likens and others, 1977). Mean air temperatures are 19°C in July and -9°C in January (Federer and others, 1990). At the Forest Service station about 500 m west of Mirror Lake (fig. 2), the average precipitation from 1978 to 1986 was 124 cm/year (Federer and others, 1990). Monthly precipitation is fairly uniform throughout the year. Typically, 8 to 12 cm of rain or snow falls each month. A continuous snowpack that is as much as 1.5 m deep accumulates each winter.

PREVIOUS AND RELATED STUDIES

As of 1996, findings from U.S. Geological Survey studies in the Mirror Lake area have been presented in reports, journal papers, and other publications. As noted above, Winter's (1984) report detailing studies from 1979 to 1983 established the basic understanding of the geohydrologic setting of Mirror Lake. Winter and others (1989) analyzed streamflow records of Streams W and NW. Rosenberry and Winter (1993) estimated the water budget of Mirror Lake. Mau and Winter (1997) estimated recharge and baseflow from streamflow hydrographs. Shattuck (1991) evaluated the effect of evapotranspiration on the interaction of ground water with Stream W. Results of borehole geophysical logging in the Mirror Lake area are reported by Paillet (1985), Hardin and others (1987), Paillet and others (1987), and Paillet and Kapucu (1989). Results of applying surface geophysical methods to detect subsurface fractures in the Mirror Lake area are reported by Haeni and others (1993) and Lane and others (1995). Harte (1992) simulated ground-water flow in a vertical section of a hillside in the study area. Hsieh and others (1993) prepared a field guide describing methods of investigations employed in the U.S. Geological Survey studies. A collection of 15 short papers describing preliminary results of fractured rock studies at the Mirror Lake area can be found in the conference proceedings edited by Morganwalp and Aronson (1996).

Research findings at the Hubbard Brook Experimental Forest are reported in numerous papers, reports, and books. A publication prepared by the U.S. Department of Agriculture Forest Service (1991) gives a selected listing. A complete list of titles up to 1991 has been compiled by Likens (1991). Some of the research results have been synthesized in three books, the latest of which is edited by Likens (1985).

ACKNOWLEDGMENTS

The authors are grateful to individuals of the U.S. Department of Agriculture Forest Service, especially Wayne Martin, Chris Eager, and the late Robert Pierce, for use of facilities at the Hubbard Brook Experimental Forest. We thank the Science Advisory Committee of the Hubbard Brook Ecosystem Study for permission to carry out drilling and field investigations. Many individuals of the U.S. Geological Survey have contributed to this study. They include Allen Shapiro, Tom Winter, Don Rosenberry, Fred Paillet, Chris Barton, Phil Harte, Carole Johnson, and Rick Perkins. Special thanks are due to property owners in the Mirror Lake area who graciously allow access to their property. Without their cooperation, data collection would have been significantly limited.

GROUND-WATER HYDROLOGY

HYDROGEOLOGIC SETTING

The two major hydrogeologic units in the Mirror Lake area are glacial deposits and crystalline bedrock (fig. 4). In addition, a layer of organic mud sediments occurs on much of the bottom of Mirror

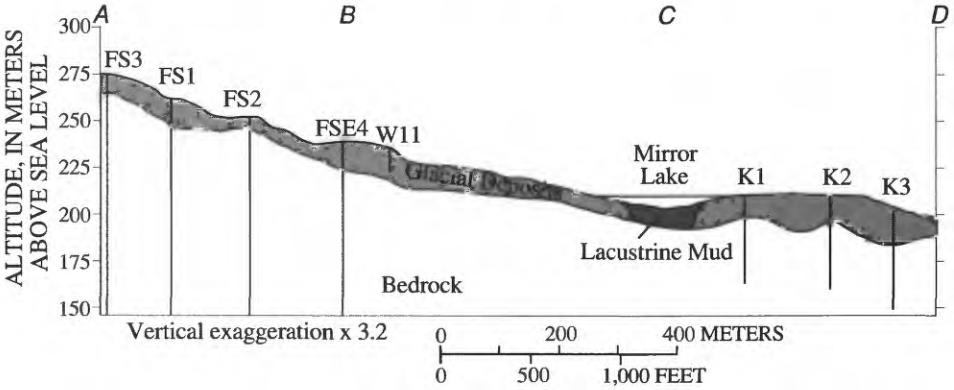

Figure 4. Hydrogeologic section A-B-C-D. (See figure 3 for location of line of section.)

Lake. Alluvium, which occurs along the Pemigewasset River, is not included in the present study.

GLACIAL DEPOSITS

Glacial deposits cover much of the land surface in the Mirror Lake area. Thickness of the glacial deposits ranges from 0 m where bedrock crops out to about 50 m at a moraine that forms the ridge north of Mirror Lake. Glacial deposits are believed to be absent from the central part of the bottom of Mirror Lake. In this area, lacustrine mud sediments are presumed to extend from lake bottom to bedrock. Thickness of glacial deposits, compiled from data provided by Winter (1984), P.T. Harte (written communications, 1994), and C.C. Barton (written communications, 1994), is shown in figure 5.

The glacial deposits consist primarily of till, but local deposits of sand and gravel are present within and overlying the till. The till is highly heterogeneous, containing clay, silt, sand, gravel, and boulders. Fine- to coarse-grained sands form kame terraces at several levels on the hillsides. A deposit of sand and gravel lies directly south of Mirror Lake, in the area between Mirror Lake and Hubbard Brook (fig 2). This deposit is believed to be a glacial delta deposit that formed when Hubbard Brook adjusted its grade to the Pemigewasset River during deglaciation (Winter, 1985). The deposit plays an important role in the hydrology of Mirror Lake, as water seeps from the lake into the highly permeable sand and gravel and flows toward Hubbard Brook.

T.C. Winter and D.O. Rosenberry (written communication, 1994) and Wilson (1991) performed slug tests (see Freeze and Cherry, 1979, p. 339) in piezometers to determine the hydraulic conductivity of the glacial deposits. Winter and Rosenberry tested 16 piezometers and analyzed their test data using the method of Bouwer and Rice (1976). Wilson tested 33 piezometers and analyzed the data using the method of Cooper and others (1967). The ranges of hydraulic conductivities determined from 15 piezometers in which slug tests were carried out in both studies are shown in table 1. Both sets of results indicate that the sand and gravel are about ten to one thousand times more permeable than the till. However, the ranges determined by Wilson are approximately three to six times the ranges determined by Winter and Rosenberry. The disagreement is probably due to different methods of analysis. In particular, the assumption of purely horizontal flow in Wilson's analysis (method of Cooper and others, 1967) might not accurately represent field conditions during the slug tests. To re-analyze some of Wilson's data,

Table 1. Ranges of hydraulic conductivities of glacial deposits as determined by slug tests.

[Hydraulic conductivity in meters per second]

Type of glacial deposit	Range of hydraulic conductivity determined by	
	Winter and Rosenberry (written communication, 1994)	Wilson (1991)
Till	2.1×10^{-7} to 1.3×10^{-6}	5.2×10^{-7} to 7.3×10^{-6}
Sand and gravel	4.6×10^{-6} to 2.9×10^{-4}	2.7×10^{-5} to 1.3×10^{-3}

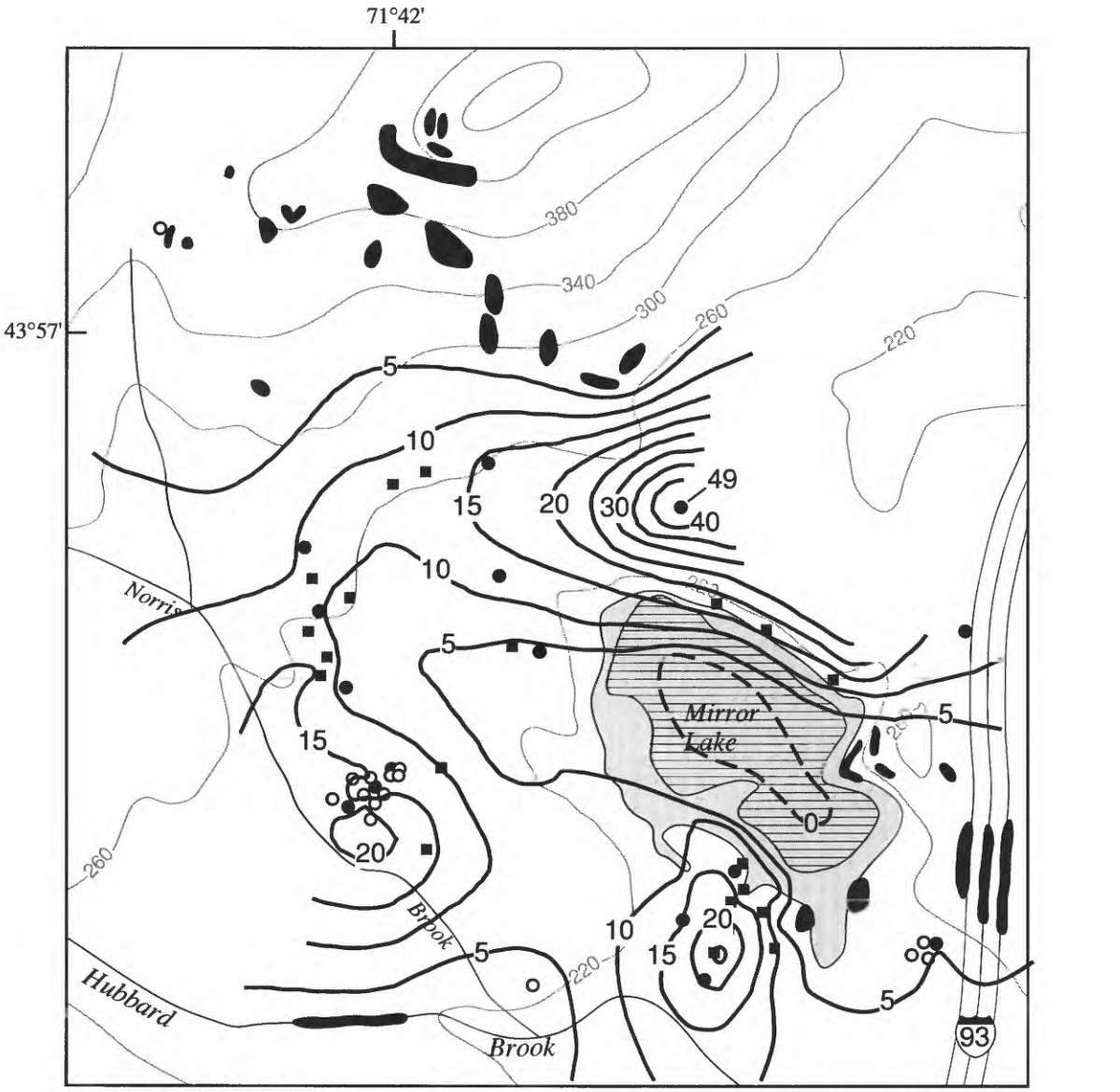

Base from U.S. Geological Survey
1:24,000 Woodstock, New Hampshire quadrangle
Land surface elevations converted from feet to meters

0 0.25 0.5 KILOMETER
0 1/4 1/2 MILE

CONTOUR INTERVAL 40 METERS

EXPLANATION

–15– LINE OF EQUAL THICKNESS OF GLACIAL DEPOSITS-Interval is 5 meters. Dashed where inferred.

AREA OF LACUSTRINE MUD SEDIMENTS

Bedrock outcrop or roadcut

Piezometer

Bedrock well and Piezometer nest

Bedrock well

Figure 5. Thickness of glacial deposits, area of lacustrine mud sediments, and areas of bedrock outcrop and roadcut in the vicinity of Mirror Lake.

Demir (1992) used a numerical model that considers both horizontal and vertical flow around the piezometer. He obtained hydraulic conductivity values that are 0.4 to 0.5 times those of Wilson. The lower values are in closer agreement with the results of Winter and Rosenberry, and are probably more representative than are Wilson's results of the glacial deposits in the Mirror Lake area.

BEDROCK

The bedrock underlying the Mirror Lake area is composed of four major rock types: schist, granite, pegmatite, and lamprophyre. The schist is part of the Rangeley formation of early Silurian age (438 to 428 million years old) (Lyons and others, 1986). It is intruded extensively by the Concord granite of late Devonian age (370 to 365 million years old). Both the schist and granite are intruded by pegmatite dikes, which are possibly a residual differentiate of the Concord granite. All three rocks are intruded by lesser amounts of lamprophyre, a fine-grained volcanic dike rock. The age of the lamprophyre is not specifically known but is likely between middle Jurassic and early Cretaceous (190 to 95 million years old), based on ages of similar dikes in the area (McHone, 1984).

The spatial distribution of rock types is highly complex. Exposed rocks on roadcuts along Interstate 93 (fig. 5) show that the bedrock composition is highly variable over distances of tens of meters. The granitic intrusions have the form of dikes, irregular pods, and anastomosing fingers, ranging from centimeters to tens of meters thick. The pegmatite and lamprophyre dikes are centimeters to meters thick. Drill cuttings and video image logs from bedrock wells show that there is generally poor correlation of rock types between adjacent wells drilled tens of meters apart. Because of these complexities, the distribution of rock type was not determined in this study. Instead, the entire bedrock complex is considered as one hydrogeologic unit.

Fractures are the major conduits through which ground water flows through the bedrock, as the intact rock has extremely low hydraulic conductivity. Barton (see Hsieh and others, 1993) mapped and analyzed fractures on road cuts along Interstate 93 and found a dominant strike in the N 30° E direction. However, fracture dips are highly variable. The granite appears more fractured than the schist. More than half of the exposed fractures have blind terminations, ending in the rock matrix without intersecting other fractures. This feature suggests that the fracture network is poorly connected.

Hydraulic conductivity of the fractured bedrock has been determined by single-well and multiple-well hydraulic tests. In a single-well hydraulic test (Hsieh and others, 1993), two packers are used to isolate a 4- to 5-m interval in a well. Hydraulic conductivity of the interval is determined by injecting or withdrawing water for approximately 20 minutes while measuring the flow rate and change in hydraulic head. Because of the relatively short test duration, these tests characterize a small volume of the bedrock within several meters of the well. Results of 208 single-well tests in the Mirror Lake area show that hydraulic conductivity of the fractured bedrock varies over at least 6 orders of magnitude, from less than 1×10^{-10} m/s (lower limit of measurement of test equipment) to 5×10^{-5} m/s. A histogram of the test results is shown in figure 6. The large range of values indicates that, at a scale of

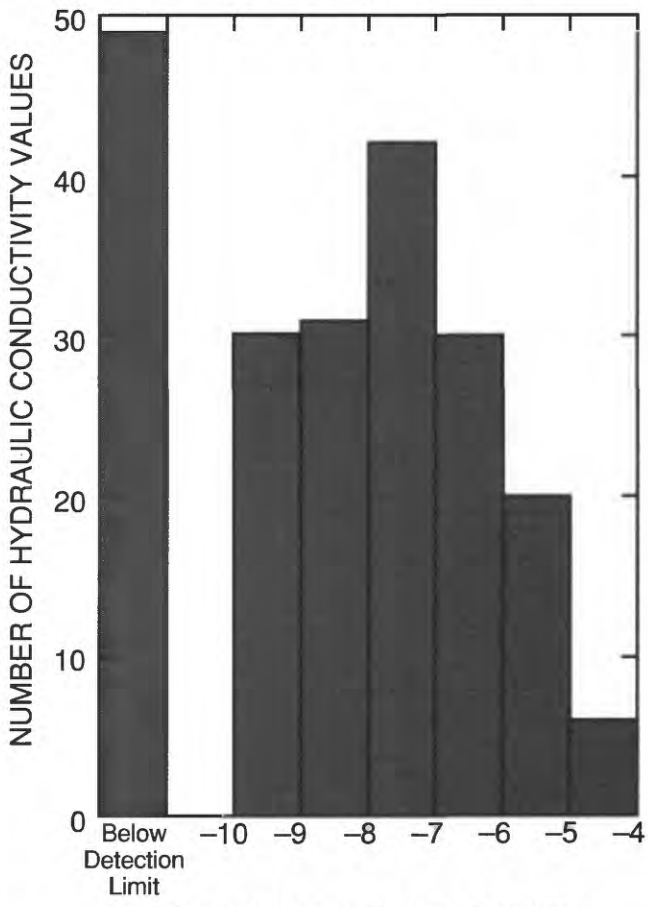

Figure 6. Histogram of hydraulic conductivities of bedrock determined by single-well hydraulic tests.

several meters, the hydraulic conductivity of the fractured bedrock is extremely heterogeneous.

In a multiple-well hydraulic test, water is withdrawn from a packer-isolated interval in one well, while changes in hydraulic head are measured in packer-isolated intervals in adjacent wells. Multiple-well hydraulic tests have been conducted at the FSE well field (fig. 3), where 13 wells were drilled in a 100-m by 100-m area. Test results indicate that the bedrock underlying the well field contains 4 highly conductive fracture clusters, each cluster occupying a near-horizontal, tabular volume approximately 1.5 m thick by 20 to 50 m in horizontal extent, and having a hydraulic conductivity of 6×10^{-5} m/s (Hsieh and Shapiro, 1994). The highly conductive fracture clusters are hydraulically connected to each other via a less conductive fracture network having horizontal and vertical hydraulic conductivities of 3×10^{-8} and 2×10^{-7} m/s, respectively. These findings suggest that, over distances of tens of meters, ground water could travel through the highly conductive fracture clusters. However, over distances of 100 m or more, ground water must flow through the less conductive fracture network. Consequently, on a scale of 100 m, the effective hydraulic conductivity of the bedrock underlying the FSE well field is strongly controlled by the less conductive fracture network. Hsieh and Shapiro (1994) estimated this effective hydraulic conductivity to be 2×10^{-7} m/s.

LAKE SEDIMENTS

Lacustrine mud sediments lie over much of the bottom of Mirror Lake. The extent of these sediments was mapped by Moeller (1978) and is shown in figure 2. The maximum thickness of the lacustrine mud is approximately 12 m (Davis and Ford, 1982). In the central part of the lake bottom, the lacustrine mud is believed to lie directly over bedrock (Rosenberry and Winter, 1993); away from the central region, the lacustrine mud overlies glacial deposits (fig. 5). Along the near-shore lake bottom (littoral zone), the lacustrine mud is absent. Hydraulic conductivity of the lacustrine mud is significantly less than that of the glacial deposits. On the basis of hydraulic properties of similar lake sediments reported in the literature (Boelter, 1972; Frape and Patterson, 1981), Rosenberry and Winter (1993) estimated the hydraulic conductivity of the Mirror Lake lacustrine mud to be between 10^{-10} to 10^{-9} m/s.

GROUND-WATER FLOW

Ground-water flow in the Mirror Lake area is typical of mountain-and-valley terrain of New England uplands. On hillsides, water from precipitation and snowmelt infiltrates to the water table, flows downslope through the saturated glacial deposits and fractured bedrock, and discharges to streams and to Mirror Lake. Along a part of the south side of Mirror Lake, lake water seeps into the subsurface and flows toward Hubbard Brook. Part of this subsurface flow discharges into a wetland that drains into the outlet stream of Mirror Lake.

RECHARGE

Recharge is the flow of water into the ground-water system, that is, the saturated zone below the water table or surface-water bodies. The three sources of recharge in the Mirror Lake area are: (1) infiltration from precipitation (including snowmelt) to the water table, (2) subsurface seepage from Mirror Lake, and (3) infiltration of stream water along losing reaches of streams. Infiltration from precipitation is the largest source of recharge. By contrast, infiltration of stream water is relatively minor and occurs only along short, local reaches of streams.

Although monthly precipitation in the Mirror Lake area is fairly uniform throughout the year, recharge from precipitation (infiltration that reaches the water table) varies seasonally. In winter, recharge is lower because infiltration from snowmelt at the base of the snowpack is minimal. In spring, recharge is greater due to rapid snowmelt and minimal evapotranspiration. In summer, recharge is lower because much of the precipitation is lost to the atmosphere by evapotranspiration from the soil zone. In late autumn, decreased evapotranspiration leads again to increased recharge. The amount of recharge from precipitation and snowmelt in the Mirror Lake area was estimated by Mau and Winter (1997) from streamflow recession analysis. Their results indicate that recharge from precipitation and snowmelt varies from 20 to 56 cm/year, or about 16 to 45 percent of precipitation.

Water seeps from Mirror Lake into the subsurface along a part of the south side of the lake. In this area, a deposit of highly permeable sand and gravel allows rapid infiltration of lake water into the ground-water system (fig. 2). On the basis of hydraulic heads

observed in piezometers and wells, hydraulic conductivities determined from slug tests, and glacial-deposit thickness inferred from seismic refraction surveys, Rosenberry and Winter (1993) estimated the seepage from Mirror Lake to be approximately 260,000 m^3/year. However, they noted that this value is subject to large uncertainty, approaching ±100 percent.

Although streams in the Mirror Lake area generally act as ground-water drains (that is, they receive ground-water discharge), stream water infiltrates into the subsurface along short, local reaches. An example of such a location is where Stream W flows near piezometer site W3 (fig. 3), at the edge of a terrace. Shattuck (1991) examined the ground-water flow pattern in this area and found that where the stream flows on till, ground water enters the stream along both its sides and its bottom. However, at a bend where the stream flows on sand, ground water enters the stream along the uphill bank, but stream water infiltrates into the ground along the downhill bank. Although the amount of stream-water infiltration is minor compared with other sources of recharge, its presence illustrates the complexity that can exist in a ground-water flow pattern on a hillside.

DISCHARGE

Ground water in the Mirror Lake area discharges to streams and to Mirror Lake. Along a stream bank, a portion of the discharge is consumed by riparian vegetation, and the remainder enters the stream to become baseflow. For Streams W, NW, and E, baseflow at the inlet to Mirror Lake represents ground-water discharge to the stream minus the sum of riparian evapotranspiration and any infiltration of stream water along losing reaches.

Baseflow in Streams W and NW at the inlet to Mirror Lake has been estimated by Mau and Winter (1997) using methods developed by the Institute of Hydrology (1980a, b) and Rutledge and Daniel (1994). They concluded that baseflow accounts for about 25 to 57 percent of streamflow. In the present study, baseflow is assumed to be 40 percent of streamflow over the long term. Long-term average streamflow (Rosenberry and Winter, 1993) and estimated long-term average baseflow in Streams W, NW, and E at their inlets to Mirror Lake are shown in table 2.

The amount of riparian evapotranspiration in the Mirror Lake area is not well known. Shattuck (1991) showed that in the summer months, riparian evapotranspiration causes diurnal variations in water levels in shallow water table wells near Stream W, but did not quantify the evapotranspiration rate. Rutledge (1993) analyzed a ten-year record of streamflow in 166 surface-water basins in the Appalachian Mountains and Piedmont area of the eastern United States, and found that for each basin, approximately 90 percent of ground-water recharge becomes baseflow in streams, while the remaining 10 percent of recharge is consumed by riparian (near-stream) evapotranspiration.

In addition to streams, Mirror Lake is also a sink for ground-water discharge. Most ground water seeps into Mirror Lake from glacial deposits along the west, north, east, and part of the south sides of the lake bottom, where the lacustrine mud sediments are absent (fig. 5). Minute amounts of ground water enter Mirror Lake by upward seepage through the lacustrine mud, or directly from bedrock where it crops out on the east side of the lake (fig. 5). Rosenberry and Winter (1993, fig. 3) estimated that ground-water seepage to Mirror Lake is approximately 80,000 m^3/year. This value, like the estimate of subsurface seepage from Mirror Lake, is also subject to large uncertainty, approaching ±100 percent.

Table 2. Long-term average streamflow and baseflow in Streams W, NW, and E at their inlets to Mirror Lake.

[Streamflow and baseflow in cubic meters per year]

Stream	Long-term average streamflow	Long-term average baseflow[1]
W	157,000	63,000
NW	249,000	100,000
E	12,000	5,000
Total	418,000	168,000

[1]Estimated as 40 percent of streamflow.

HYDRAULIC HEAD

DATA COLLECTION

Since 1979, hydraulic heads have been measured weekly in piezometers and bedrock wells in the Mirror Lake area. Piezometer and well construction are described by Winter (1984). From 1979 through 1993, about 70 piezometers having either 0.6 or 1.0 m long screens were installed in the glacial

deposits. The locations of 48 piezometers used for model calibration are shown in figure 3. Approximately half of these piezometers (those with names starting with W) are screened at or just below the water table. The remainder are grouped into nests that are installed at various depths adjacent to bedrock wells. The names of these piezometers consist of the bedrock well name and a suffix equal to the depth of the screen midpoint, in feet below land surface. Hydraulic head in a piezometer is assumed to represent hydraulic head at the midpoint of the piezometer screen. Altitudes of the piezometer screen midpoints are given in table 3. The depths of the screen midpoints range from 1 m to 40 m below land surface.

From 1979 through 1993, 30 bedrock wells were installed in the Mirror Lake area. Depths of wells range from 46 m to 305 m below land surface. Of the 30 wells, 13 are clustered in a 100 m by 100 m area known as the FSE well field, 4 are clustered in another 100 m by 100 m area known as the CO well field, and the remainder are distributed over a 1 km by 1 km area in the vicinity of Mirror Lake (fig. 3). Prior to 1989, hydraulic heads were measured in open bedrock wells. Since 1989, inflatable packers have been installed in many of the bedrock wells to allow multi-level monitoring (Hsieh and others, 1996). Packers are positioned in a well to hydraulically isolate high transmissivity fractures from each other. Hydraulic head in a packer-isolated interval is assumed to represent hydraulic head in the

Table 3. Altitude of screen midpoint, long-term average hydraulic head, and averaging method for piezometers.

[Altitude and hydraulic head in meters above sea level]

Piezometer	Altitude of screen midpoint	Long-term average hydraulic head	Averaging method
CO1-11	214.3	215.71	1991 adjusted
CO1-18	211.8	215.52	1991 adjusted
FS1-17	255.7	259.62	Direct
FS1-25	253.9	259.90	Direct
FS1-35	250.9	260.81	Direct
FS3-11	271.0	271.53	Direct
FS3-22	267.6	271.13	Direct
FS3-29	265.5	270.48	1991 adjusted
FSE2-23	233.5	234.40	Direct
FSE2-43	226.8	234.14	Direct
FSE5-36	231.3	237.30	Dec 93 adjusted
FSE6-41	229.8	237.57	1991 adjusted
FSE6-59	224.3	237.36	1991 adjusted
IS1-18	220.0	221.70	Dec 93 adjusted
IS1-38	213.1	221.81	Dec 93 adjusted
K1-8	211.8	212.78	Direct
K1-39	202.3	211.82	Direct
K2-21	208.4	210.40	Direct
K2-41	202.3	210.48	Direct
K3-22	200.5	207.08	Direct
K3-61	188.6	205.78	Direct
R1-36	246.0	249.15	1993 adjusted
R1-55	239.9	250.71	1993 adjusted
TR1-63	229.8	233.90	Direct
TR1-132	208.2	233.02	1991 adjusted
TR2-23	225.9	232.09	1993 adjusted
W2	251.9	252.08	Direct
W3	251.5	257.84	Direct
W3A	256.0	257.10	Direct
W5	209.6	210.69	Direct
W6	228.4	231.70	Direct
W7	212.3	212.94	Direct
W8	212.3	212.77	Direct
W9	211.8	212.45	Direct
W10	209.6	211.22	Direct
W11	232.4	234.11	Direct
W13	209.5	210.09	Direct
W14	207.1	207.25	Direct
W15	261.0	261.86	Direct
W16	257.9	262.33	Direct
W18	227.1	227.78	Direct
W19	214.0	214.19	Direct
W20	213.6	213.77	Direct
W21	214.2	213.95	Direct
W24	208.5	208.52	1991 adjusted
W25	254.5	256.70	1991 adjusted
W26	251.5	252.72	1991 adjusted
W27	262.4	263.23	1991 adjusted

most transmissive fracture of the interval. This assumption is reasonable because the most transmissive fracture in an interval is typically at least one order of magnitude more transmissive then the other fractures in the interval. Consequently, hydraulic head in the most transmissive fracture dominates hydraulic head in the interval. Locations of packer-isolated intervals in each well, and the positions of the most transmissive fracture in each interval are shown in table 4. In each well, packer-isolated intervals are named in alphabetical order, beginning with the uppermost interval. For example, the three intervals of well FS1 are denoted, from top to bottom, as FS1-a, FS1-b, and FS1-c. An interval name without a trailing letter denotes a well without packers. In this case, the interval is the entire open-hole section of the well.

In September 1995, an additional bedrock well, FS7, was drilled on the ridge near the northwest corner of the study area (fig. 1). This well provides a hydraulic head measurement near the highest altitudes of the Mirror Lake area, where hydraulic head data were heretofore unavailable due to limited drilling access. Because the well was drilled near the end of this modeling study, hydraulic head measured in the well was not used in calibration runs completed prior

Table 4. Altitude of top, bottom, and most transmissive fracture; long-term average hydraulic head; and averaging method for well intervals .

[Altitude and hydraulic head in meters above sea level]

Well interval	Altitude at top of interval	Altitude at bottom of interval	Altitude of most transmissive fracture	Long-term average hydraulic head	Averaging method
CO1-a	208	166	184	216.29	1991 adjusted
CO1-b	165	41	88	215.07	1991 adjusted
CO2-a	209	184	209	215.38	1991 adjusted
CO2-b	183	155	166	216.66	1991 adjusted
CO3-a	208	189	205	214.16	1991 adjusted
CO3-b	189	175	185	215.75	1991 adjusted
FSE1-a	223	208	222	233.97	1991 adjusted
FSE1-b	207	174	194	233.83	1991 adjusted
FSE1-c	173	131	140	235.43	1991 adjusted
FSE2-a	224	208	222	233.99	1991 adjusted
FSE2-b	208	174	202	233.81	1991 adjusted
FSE2-c	174	132	172	235.61	1991 adjusted
FSE3-a	223	208	222	233.95	1991 adjusted
FSE3-b	208	174	192	233.79	1991 adjusted
FSE3-c	174	132	143	236.99	1991 adjusted
FSE4-a	223	209	215	233.83	1991 adjusted
FSE4-b	208	175	197	233.83	1991 adjusted
FSE4-c	174	135	140	237.13	1991 adjusted
FSE4-d	134	11	107	240.42	1991 adjusted
FSE5	225	181	207	233.84	1991 adjusted
FSE6-a and b[1]	220	166	210	235.52	1991 adjusted
FSE7	224	166	222	235.00	Dec 93 adjusted
FSE8-a	221	190	211	234.87	Dec 93 adjusted
FSE8-b	190	166	167	234.97	Dec 93 adjusted
FSE9-a	223	198	200	234.99	Dec 93 adjusted
FSE9-b	197	166	177	234.98	Dec 93 adjusted
FSE10-a	222	212	216	235.65	Dec 93 adjusted

Table 4. Altitude of top, bottom, and most transmissive fracture; long-term average hydraulic head; and averaging method for well intervals—Continued.

[Altitude and hydraulic head in meters above sea level]

Well interval	Altitude at top of interval	Altitude at bottom of interval	Altitude of most transmissive fracture	Long-term average hydraulic head	Averaging method
FSE10-b	211	168	208	235.32	Dec 93 adjusted
FSE11-a	218	184	197	234.98	Dec 93 adjusted
FSE11-b	183	158	163	235.00	Dec 93 adjusted
FSE12-a	223	179	187	235.34	Dec 93 adjusted
FSE12-b	178	156	158	236.40	Dec 93 adjusted
FSE13-a	216	199	203	234.91[1]	Dec 93 adjusted
FSE13-b	198	164	193		
FS1-a	245	229	235	256.15[1]	1991 adjusted
FS1-b	229	196	223		
FS1-c	195	124	166	256.50	1991 adjusted
FS2-a	246	223	226	247.32	1991 adjusted
FS2-b	223	190	212	247.59	1991 adjusted
FS2-c	189	103	135	240.92	1991 adjusted
FS3-a	262	248	253	269.13	1991 adjusted
FS3-b	247	215	244	268.43	1991 adjusted
FS3-c	214	48	162	265.05	1991 adjusted
FS4	343	45	not known	350.54	Dec 93 adjusted
FS7	660 (approx.)	610 (approx.)	not known	650 (approx.)	single measurement, Sept 95
H1-a	223	193	198	220.86	1993 adjusted
H1-b	192	159	176	218.50	1993 adjusted
H1-c	159	140	155	220.24	1993 adjusted
IS1-a	208	203	207	221.60	1993 adjusted
IS1-b	202	150	151	219.28	1993 adjusted
IS1-c	149	72	101	217.63	1993 adjusted
K1	200	168	not known	212.65	Direct
K2	198	166	not known	211.04	Direct
K3	186	154	not known	208.34	Direct
R1-a	237	226	234	250.06	1993 adjusted
R1-b	225	192	221	250.06	1993 adjusted
R1-c	192	63	109	251.39	1993 adjusted
T1-a	223	197	208	224.95	1993 adjusted
T1-b	196	169	179	224.79	1993 adjusted
T1-c	169	76	161	224.90	1993 adjusted
TR1-a	197	188	194	231.10	1991 adjusted
TR1-b	187	157	163	228.96	1991 adjusted
TR1-c	157	58	101	225.72	1991 adjusted
TR2-a	217	199	201	233.02	1993 adjusted
TR2-c	165	1	148	233.50	1993 adjusted

[1]Two intervals combined into one due to failure of packer to hydraulically isolate the two intervals.

to September 1995. Instead, an additional calibration run was carried out to include the new data.

TEMPORAL VARIATION OF HYDRAULIC HEAD

Hydraulic head in glacial deposits and bedrock of the Mirror Lake area exhibits both seasonal and shorter-period variations. To illustrate these variations, hydrographs from 1991 through 1993 in piezometer FS1-17 and in packer-isolated intervals of bedrock well FS3 are shown in figure 7. Seasonal variation in these hydrographs is caused by the seasonal variation in recharge from precipitation. In spring, hydraulic head typically rises to an annual

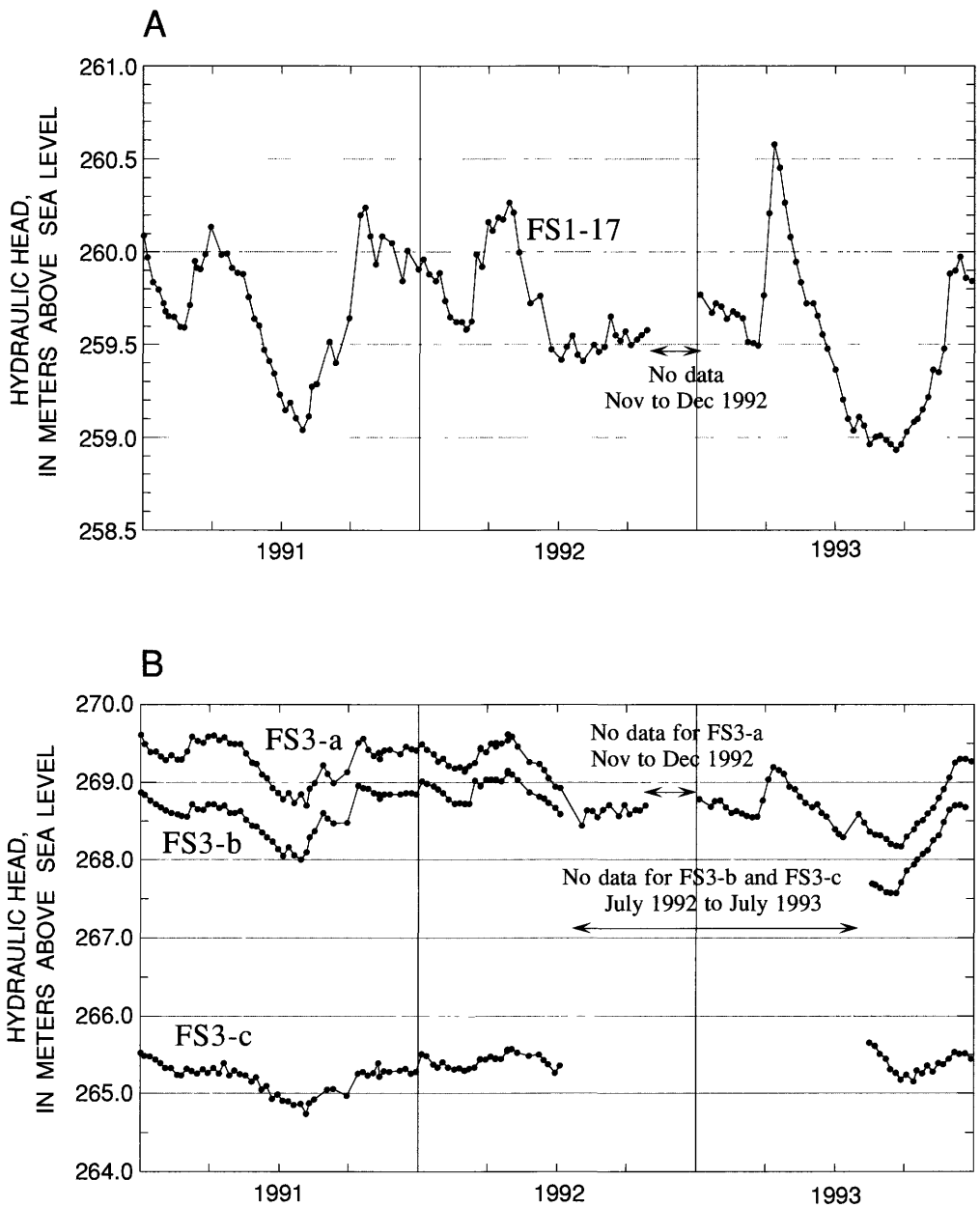

Figure 7. Hydraulic head from 1991 through 1993 in piezometer FS1-17 (A) and in packer-isolated intervals of bedrock well FS3 (B).

maximum due to high recharge from snowmelt and rainfall. In summer, hydraulic head declines because of lower recharge caused by increased evapotranspiration. In autumn, hydraulic head usually rises again, as evapotranspiration decreases, and typically reaches a peak that is smaller than the spring peak. In winter, hydraulic head generally declines due to lower recharge, but might also rise if mild temperatures in midwinter melt some of the snowpack. Superimposed on the seasonal variation in hydraulic head are shorter-period variations that are due to individual periods of precipitation and snowmelt.

LONG-TERM AVERAGE HYDRAULIC HEAD

The steady-state flow model developed in this study is designed to simulate long-term average flow conditions. Therefore, the model should be calibrated to long-term average hydraulic heads. Because data have been collected in piezometers and wells over varying durations, two different methods are used to determine long-term averages. The results are given in tables 3 and 4.

For piezometers and wells that have five or more years of hydraulic-head measurements, a "direct" method is used to determine long-term averages. This method involves first computing the annual average hydraulic head for all calendar years in which there are at least 26 weekly measurements. Then the long-term average hydraulic head is computed as the average of the annual averages. This method is denoted as "Direct" in tables 3 and 4.

For piezometers and wells that have less than 5 years of hydraulic-head measurements, an "adjustment" method is used to estimate long-term averages. In many cases, data are sufficient to determine the annual average hydraulic head only for 1991. Because this annual average might not be representative of the long-term average, an adjustment is applied. The adjustment is based on a best-fit, linear relation between the 1991 annual average hydraulic head and the long-term average hydraulic head for wells and piezometers for which both averages can be calculated. This linear relation is then used to estimate the long-term average hydraulic heads in cases where data are sufficient to determine only the 1991 annual average hydraulic head. This method is denoted by "1991 adjusted" in tables 3 and 4. A similar method is applied to a few cases for which data are sufficient to determine only an annual average hydraulic head for 1993, or a monthly average hydraulic head for December 1993. The latter methods are denoted respectively by "1993 adjusted" and "Dec 93 adjusted" in tables 3 and 4.

The long-term average altitude of the water table as determined from the long-term average hydraulic head data is shown in figure 8. The water table is generally within 20 m of land surface, and in many locations, less than 10 m below land surface. Hydraulic head measured at the newly drilled well FS7 indicates that the water table may remain shallow all the way to the highest altitude at the northwest corner of the study area. Near this ridge top, hydraulic head in well FS7 is approximately 15 m below land surface.

The distribution of long-term average hydraulic heads in the vertical section A-B through four wells on a hillside west of Mirror Lake (see fig. 8) is shown in figure 9. Although the hydraulic gradient indicates a predominance of lateral flow in the downhill direction, vertical components of flow are also apparent. Ground water flows downward from glacial deposits to bedrock along most of the section from well FS3 to well FS2. Near FSE4, however, upward flow is significant in the bedrock.

MODEL OF STEADY-STATE GROUND-WATER FLOW

Ground-water flow in the glacial deposits and crystalline bedrock of the Mirror Lake area is simulated by the U.S. Geological Survey Modular Three-Dimensional Finite-Difference Ground-Water Flow Model (McDonald and Harbaugh, 1988), commonly known as MODFLOW. The steady-state model in this study simulates long-term average flow conditions. Seasonal and shorter-period variations are not considered. Because MODFLOW is a continuum model, its application to fractured rock presupposes that the rock can be treated as an equivalent porous medium.

ASSUMPTIONS

The model developed in this study is based on four simplifying assumptions. These assumptions are: (1) recharge from precipitation is areally uniform,

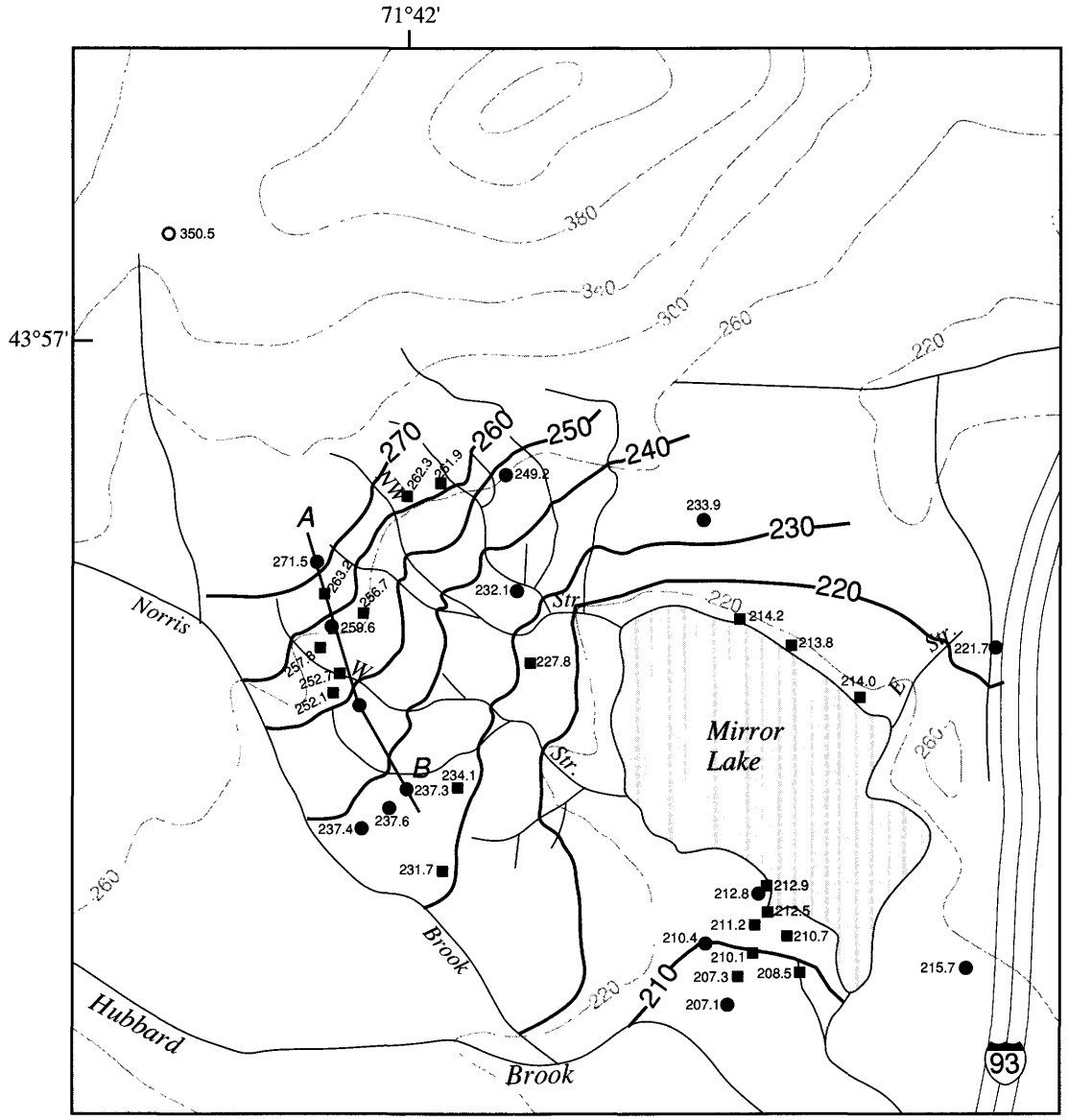

Base from U.S. Geological Survey
1:24,000 Woodstock, New Hampshire quadrangle
Land surface elevations converted from feet to meters

0 0.25 0.5 KILOMETER
0 1/4 1/2 MILE

TOPOGRAPHIC CONTOUR INTERVAL 40 METERS

EXPLANATION

211.2 ■ PIEZOMETER

237.4 ● BEDROCK WELL AND PIEZOMETER NEST

350.5 O BEDROCK WELL FS4

Number adjacent to symbol indicates long-term average altitude of water table, in meters above sea level.

—230— WATER TABLE CONTOUR-Shows long-term average altitude of water table. Contour interval 10 meters. Datum is sea level

A—B LINE OF HYDROLOGIC SECTION (See fig. 9)

Figure 8. Long-term average altitude of water table in the vicinity of Mirror Lake.

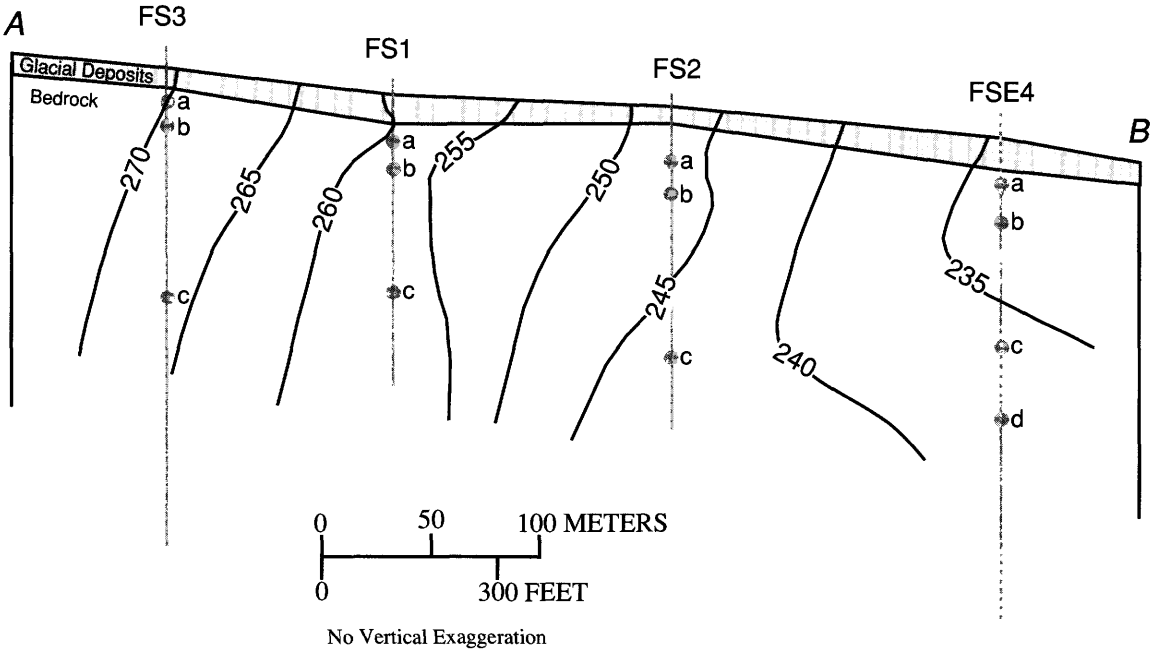

EXPLANATION

—240— HYDRAULIC HEAD CONTOUR-Shows long-term average hydraulic head. Contour interval 5 meters. Datum is sea level.

a HYDRAULIC HEAD MEASUREMENT LOCATION-Denotes well interval and location of the highest-transmissivity fracture in the well interval.

Figure 9. Long-term average hydraulic heads in section A-B. (See figure 8 for location of line of section.)

(2) riparian evapotranspiration is a small component of ground-water discharge to streams and can be neglected, (3) flow in the bedrock occurs primarily in the uppermost 150 m, and (4) the distribution of hydraulic conductivity can be represented by dividing the model domain into several zones each having uniform properties.

The assumption of spatially uniform recharge from precipitation is adopted because of the lack of more detailed information. Although variations in precipitation, slope, vegetation, and soil could lead to variations in infiltration, studies of such spatial variability have not been carried out in the Mirror Lake area. To the extent that recharge from precipitation is assumed uniform in the model, the simulation results might not accurately represent local details in the ground-water system. However, if the recharge variability is not great, then the simulation results should provide a useful characterization of the overall ground-water system and ground-water budget.

The assumption of negligible riparian evapotranspiration is based on the work of Rutledge (1993), who estimated that for several surface-water basins in the Appalachians and Piedmont, approximately 10 percent of recharge to ground water is consumed by riparian evapotranspiration, and the remaining 90 percent of recharge becomes baseflow in streams. In the model of ground-water flow in the Mirror Lake area, riparian evapotranspiration is neglected. Therefore, at the inlet to Mirror Lake, it is assumed that baseflow in the W, NW, or E Stream equals ground-water discharge to the stream less any infiltration of stream water along losing reaches.

The assumption that flow in the bedrock occurs primarily in the uppermost 150 m is based on results of hydraulic tests using packers to determine the hydraulic conductivity distribution in wells to depths of about 250 m. The test results indicate that most of the permeable fractures are within 150 m of the bedrock surface. Although permeable fractures are

present at greater depths, they are relatively uncommon. By limiting ground-water flow in the bedrock to the uppermost 150 m, the model in this study ignores the possibility of deeper ground-water flow at larger regional scales that extend beyond the study area.

The distribution of hydraulic conductivity in the model is represented by a "zonation" approach. In this approach, the model domain is divided into several zones. Within each zone, hydraulic conductivity is uniform but can be isotropic or anisotropic. The zones and the associated hydraulic conductivities define the "parameter structure." The parameter structure characterizes the large-scale variation of hydraulic conductivity in the model domain. Variations on scales smaller than the zone dimension are neglected. Consequently, the simulation results characterize the overall ground-water system, but not local details.

GOVERNING EQUATION

In the absence of internal sources and sinks, the equation of three-dimensional, steady-state ground-water flow is (Freeze and Cherry, 1979, p. 64):

$$\frac{\partial}{\partial x}\left(K_H\frac{\partial h}{\partial x}\right)+\frac{\partial}{\partial y}\left(K_H\frac{\partial h}{\partial y}\right)+\frac{\partial}{\partial z}\left(K_V\frac{\partial h}{\partial z}\right)=0\,, \quad (1)$$

where

h = hydraulic head (L),
K_H = horizontal hydraulic conductivity (L/T),
K_V = vertical hydraulic conductivity (L/T),
x, y = cartesian coordinates in the horizontal directions (L),
z = cartesian coordinate in the vertical direction (L).

Implicit in equation 1 is the assumption that two principal directions of hydraulic conductivity are horizontal and the third is vertical. Hydraulic conductivity is isotropic in the horizontal plane, but could exhibit horizontal-to-vertical anisotropy. In the model, hydraulic conductivities of the different zones are designated by additional subscripts.

Equation 1 is solved using MODFLOW with the preconditioned conjugate gradient method (PCG2) (Hill, 1990). The MODFLOW computer code is modified slightly so that the drying of finite-difference cells is delayed until the iterative solution loop is exited. During the solution loop, if the saturated thickness of a cell becomes zero, the horizontal hydraulic conductivity is set to zero, but the vertical hydraulic conductivity is not changed. This modification allows cells to become resaturated from below. When the solution loop is exited, cells with saturated thickness equal to zero are removed. If the PCG2 solver has not converged, additional passes through the iterative solution loop, with delayed drying of cells, are performed until convergence is achieved.

SPATIAL DISCRETIZATION

The three-dimensional model domain extends horizontally over the Mirror Lake area and vertically from the water table to 150 m below the bedrock surface. In the horizontal dimensions, the model domain is discretized into a grid of 89 rows by 85 columns of rectangular cells (fig. 10). The central part of the grid has square cells 17 m on each side. Outside the central part, cell dimension increases towards the perimeter in two stages, from 17 m to 50 m, and then from 50 m to 150 m. The finer, central part of the grid allows more accurate model simulation in the area of focused investigation near Mirror Lake. The coarser, outer part of the grid allows coverage of the entire study area using a reasonable number of cells.

In the vertical dimension, the model domain is discretized into five model layers. The upper two model layers (layers 1 and 2) represent glacial deposits, Mirror Lake, the lacustrine mud sediments, and the Pemigewasset River. The lower three model layers (layers 3, 4 and 5) represent the bedrock. Conceptually, the five model layers slope with the land surface as illustrated by the vertical section along row 25 of the model grid (fig. 11). In the actual MODFLOW simulation, the layer slope is ignored, and thus an error is introduced. However, Harte (1994) investigated the magnitude of this error and found it to be relatively small.

In the central part of the grid where the thickness of glacial deposits is known (fig. 5), layers 1 and 2 are each assigned half the thickness of the glacial deposits. In the outer part of the grid where the thickness of glacial deposits is unknown, layers 1 and 2 are each assigned a uniform thickness of 4.5 m. Where bedrock crops out, layers 1 and 2 are absent. Mirror Lake is represented by cells in layer 1, and the lacustrine mud sediments are represented by cells in

layer 2. As shown in figure 12, the lacustrine mud is assumed to lie directly on bedrock. This approximation ignores the fringe region where these sediments overlie glacial deposits. The Pemigewasset River is represented by the eastern-most cell of each model row in layer 1 (figure 10). The bedrock is represented by the lower three model layers (layers 3, 4, and 5). The top of layer 3 is the bedrock surface, and the bottom of layer 5 is 150 m below the bedrock surface. Each of layers 3, 4, and 5 has a uniform thickness that is respectively 30 m, 60 m, and 60 m.

BOUNDARY CONDITIONS

The vertical surfaces that bound the sides of the model domain are specified as no-flow boundaries (fig. 10). On the east, north, and west sides, these vertical boundary surfaces approximately lie beneath the Pemigewasset River, Leeman's Brook, Paradise Brook, and a reach of Hubbard Brook. The no-flow boundary condition beneath these water bodies is a result of the assumption that ground water does not flow across the river and streams, but discharges into them. On the south side and near the northwest corner of the model domain, the vertical boundary surfaces lie beneath major topographic divides. The no-flow boundary condition in these areas is a result of the assumption that the topographic divides are also ground-water divides. The bottom surface of the model domain (150 m below bedrock surface) is also specified as a no-flow boundary. The use of this boundary condition ignores ground water flow in the bedrock at depths greater than 150 m below the bedrock surface.

Mirror Lake and the Pemigewasset River are both represented in layer 1 by cells that are assigned known hydraulic heads. Cells representing Mirror Lake are assigned a hydraulic head of 213 m above sea level, which is the average lake surface altitude from 1982 through 1990. Cells representing the Pemigewasset River are assigned a hydraulic head of 177 m above sea level, which is the river stage obtained from the U.S. Geological Survey Woodstock topographic map (7-1/2 minute series). The small gradient in the river stage over the study area is neglected. The use of constant-head cells to represent Mirror Lake and the Pemigewasset River precludes determination of a water balance for these surface water bodies.

The position of the water table is not specified but is computed in the model simulation. At each model cell in the horizontal dimension, the computed water table may lie in any of the five model layers. During the simulation, model cells that lie above the water table become "inactive" and are eliminated from the simulation. Model cells that contain or lie below the water table remain "active" in the simulation.

Recharge from precipitation is represented as an areally uniform flux applied to the uppermost active cell throughout the model domain, except for cells representing Mirror Lake. At these lake cells, precipitation enters the lake, and there is no direct recharge to the ground-water system. The rate of recharge from precipitation is estimated during model calibration.

Streams in the model domain include Hubbard Brook, Norris Brook, Paradise Brook, Leeman's Brook, Streams W, NW and E, and their tributaries. In the context of the present ground-water flow model, streams are defined as locations where the topography forms a stream channel, regardless of whether or not flow is perennial in the channel. Therefore, certain stream segments in the ground-water model might not qualify as streams on a topographic map. The amount of ground-water discharge into a stream is determined by model simulation.

Streams are simulated in the model by the Streamflow Routing Package of MODFLOW, which simulates the interaction between streams and ground water, and accounts for the amount of flow in streams (Prudic, 1989). In this approach, streams are considered to lie over model cells in layer 1. Each stream is divided into many reaches, each reach corresponding to an individual model cell over which the stream traverses (fig. 10). For a reach, flow from the underlying model cell to the stream is computed by (Prudic, 1989, p. 7):

$$Q_s = C_s (H_s - h) , \qquad (2)$$

where

C_s = streambed conductance (L^2/T),
H_s = average stream stage in the reach (L), and
h = hydraulic head in the cell (L).

The average stream stage is determined from the topographic map of the Mirror Lake area. If the average stage of a reach is lower than the hydraulic

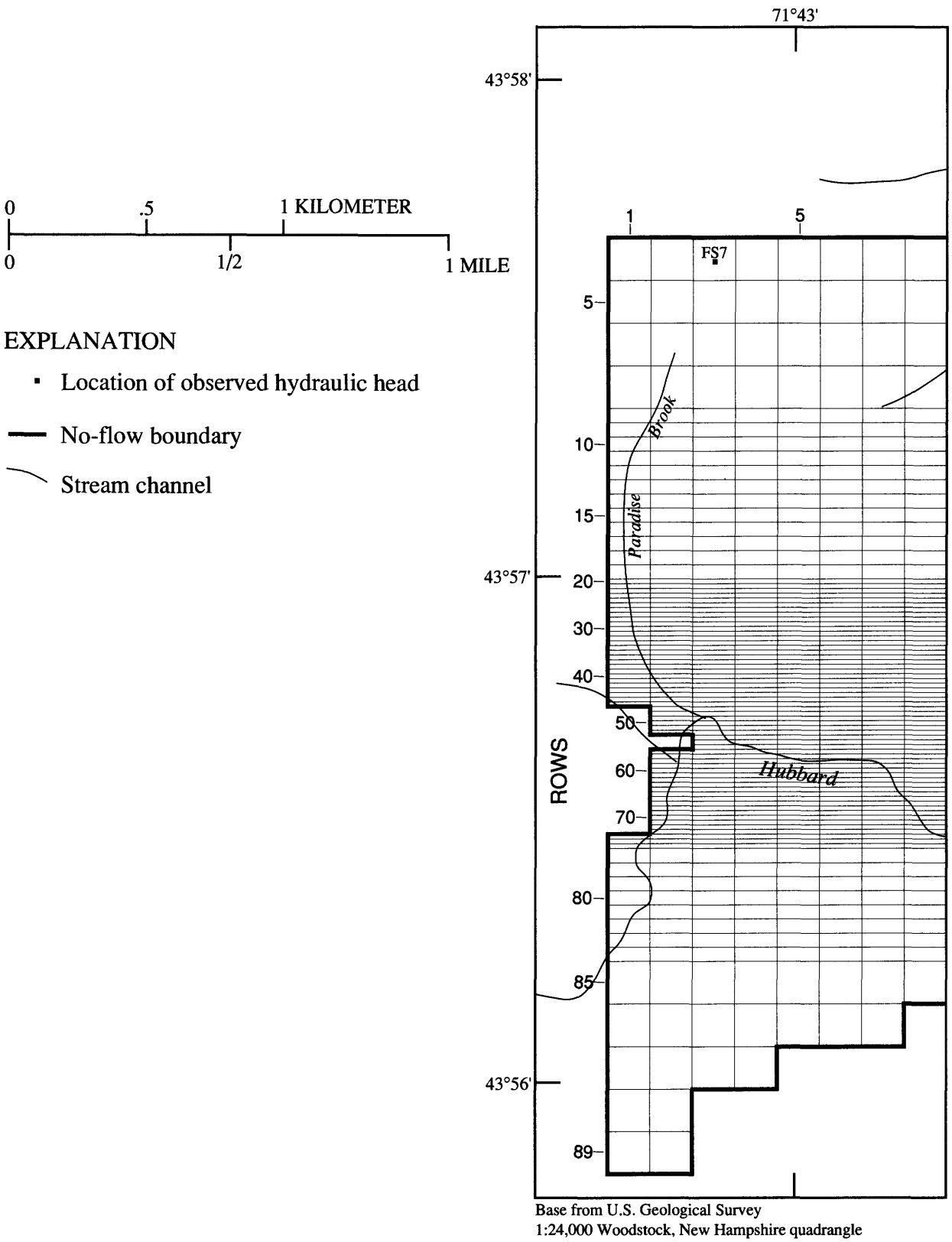

Base from U.S. Geological Survey
1:24,000 Woodstock, New Hampshire quadrangle

Figure 10. Model grid and boundary conditions.

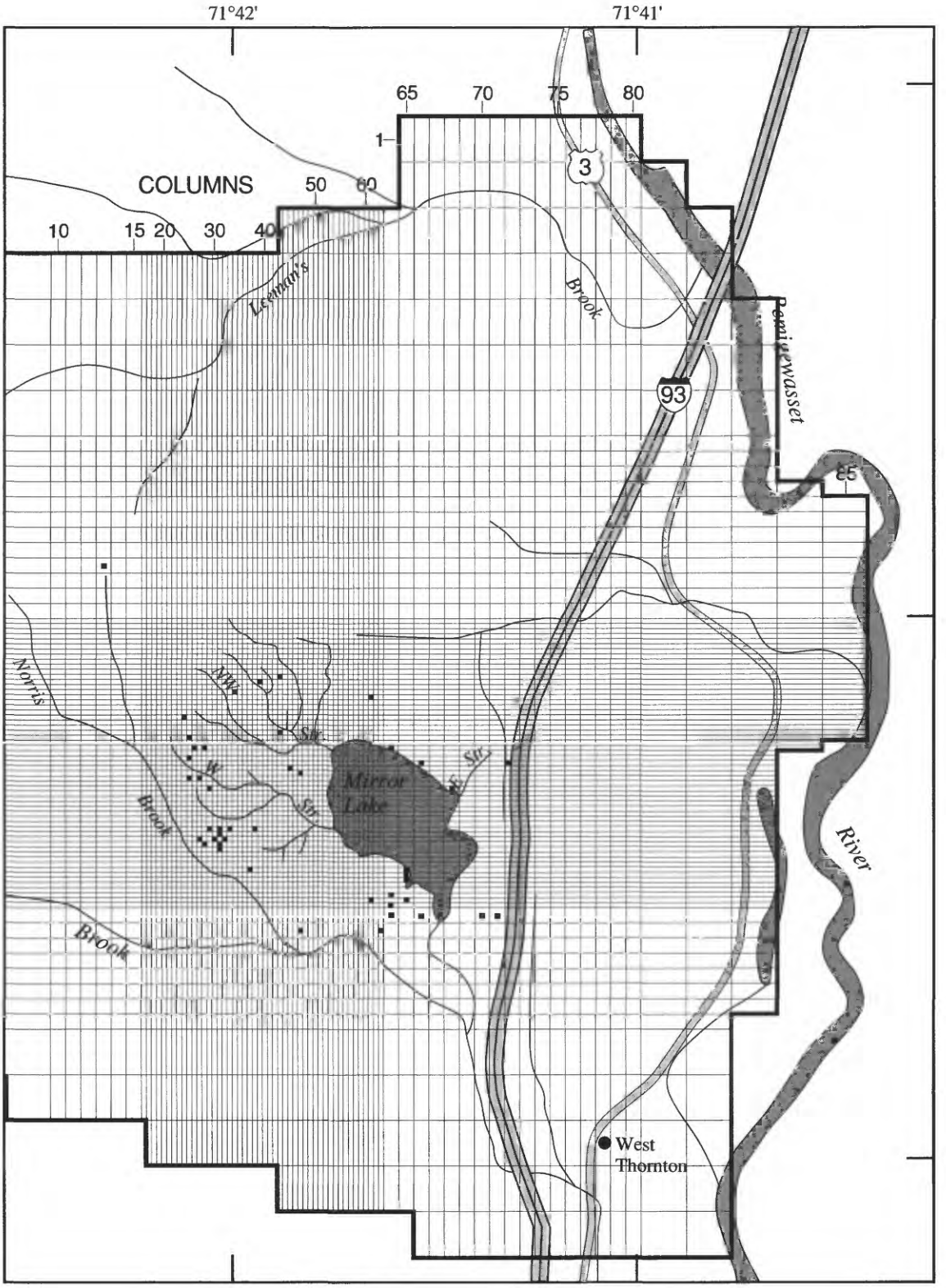
71°42'
71°41'
COLUMNS
1
10
15
20
30
40
50
60
65
70
75
80
85
3
93
Leeman's
Brook
Pemigewasset
River
Norris
Brook
Mirror
Lake
West
Thornton

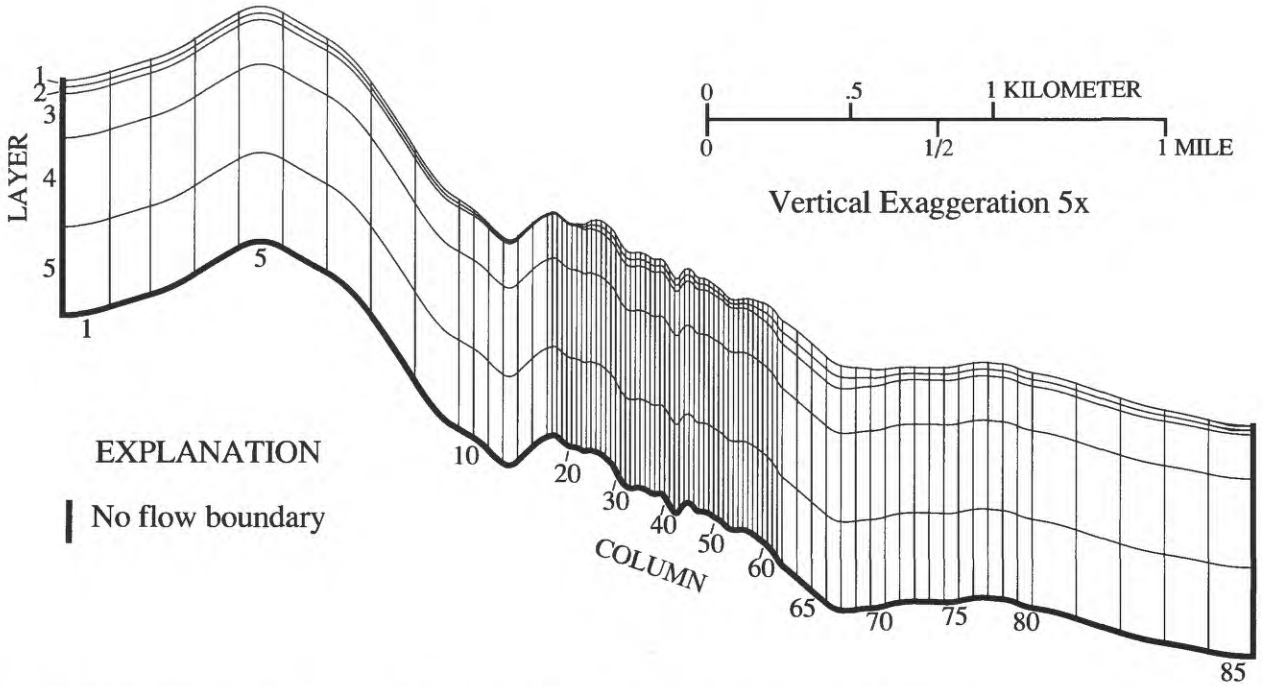

Figure 11. Section along row 25 of the model grid showing the five model layers.

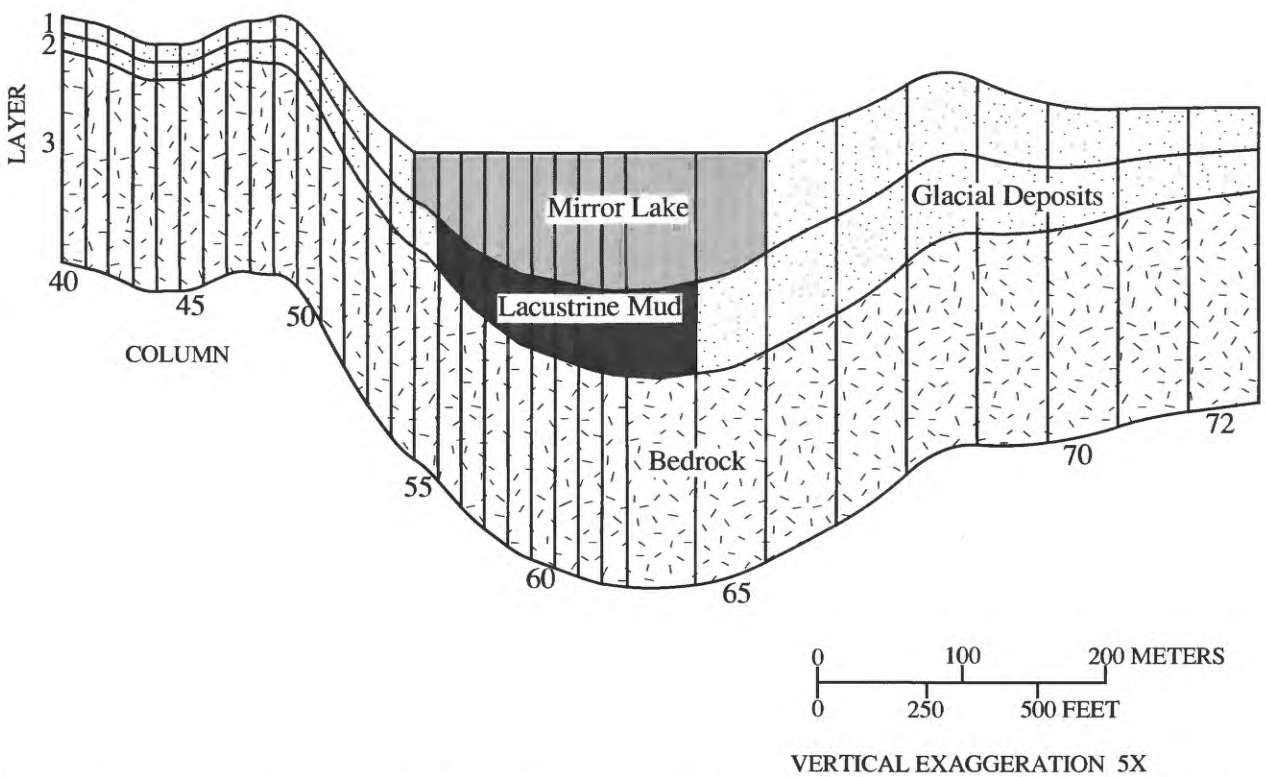

Figure 12. Section along row 50 of the model grid showing glacial deposits, Mirror Lake, lacustrine mud sediments, and bedrock in layers 1, 2, and 3.

head in the underlying model cell, ground water discharges into the stream (Q_s is negative). Conversely, if the average stage of a reach is higher than the hydraulic head in the underlying model cell, stream water infiltrates into the ground-water system (Q_s is positive), providing there is streamflow in the reach. After Q_s is computed for a reach, it is added to the streamflow from the adjacent upstream reach, and the sum is routed to the adjacent downstream reach. Because the streamflow simulated in this manner is derived from ground-water discharge, it represents baseflow in the stream.

In theory, the streambed conductance can be determined by (Prudic, 1989, p. 7)

$$C_s = \frac{K_s W_s L_s}{B_s}, \qquad (3)$$

where

K_s = hydraulic conductivity of the stream bed (L/T),
B_s = thickness of the streambed (L),
W_s = width of the stream reach (L), and
L_s = length of the stream reach (L).

In the present study, K_s and B_s are not known, so equation 3 cannot be directly applied. However, work of Shattuck (1991) indicates that there is little resistance to flow between the glacial deposits and the streams in the Mirror Lake watershed; that is, streambed conductance is high. Therefore, the streambed conductance is set to a large value for all stream reaches. This approach causes hydraulic heads in the cells below the streams to be nearly the same as the stream stage, in areas of the model where the computed Q_s is not zero.

PARAMETER STRUCTURE

Distribution of hydraulic conductivity in the model is represented by dividing the model domain into zones, each having homogeneous hydraulic conductivity. The zones and hydraulic conductivities together define the parameter structure. Four different parameter structures are considered for the ground-water flow model of the Mirror Lake area. Model calibration is carried out for each parameter structure.

The simplest parameter structure is referred to as parameter structure A (table 5). The zones for this parameter structure correspond to the three hydrogeo-

Table 5. Hydraulic conductivities used in parameter structures A, B, C, and D.

[Hydraulic conductivity in meters per second; estimated, value estimated during model calibration; --, not used in parameter structure]

Hydraulic conductivity parameter	Value in parameter structure			
	A	B	C	D
Glacial Deposits (excluding sand and gravel south of Mirror Lake)				
K_{GD}	estimated	--	estimated	estimated
$K_{GD,H}$	--	estimated	--	--
$K_{GD,V}$	--	$K_{GD,H}/10$	--	--
Sand and Gravel south of Mirror Lake				
K_{SG}	5×10^{-5}	5×10^{-5}	5×10^{-5}	5×10^{-5}
Lacustrine Mud Sediments				
K_{LM}	1×10^{-9}	1×10^{-9}	1×10^{-9}	1×10^{-9}
Bedrock				
K_{BR}	estimated	estimated	--	--
$K_{BR,3}$	--	--	estimated	--
$K_{BR,4}$	--	--	estimated	--
$K_{BR,5}$	--	--	estimated	--
$K_{BR,U}$	--	--	--	estimated
$K_{BR,L}$	--	--	--	estimated

logic units in the Mirror Lake area (glacial deposits, lacustrine mud, and bedrock), with one exception. Because the sand and gravel south of Mirror Lake (fig. 2) exert an important control on the subsurface seepage from the lake, this deposit is considered a separate zone from the rest of the glacial deposits. Therefore, the zonation scheme for parameter structure A divides the model domain into four zones: glacial deposits, sand and gravel, lacustrine mud, and bedrock. The hydraulic conductivity of each zone is assumed to be isotropic. The hydraulic conductivities in parameter structure A are:

K_{GD} = hydraulic conductivity of glacial deposits, excluding sand and gravel south of Mirror Lake (L/T),

K_{SG} = hydraulic conductivity of sand and gravel south of Mirror Lake (L/T),

K_{LM} = hydraulic conductivity of lacustrine mud sediments (L/T), and

K_{BR} = hydraulic conductivity of bedrock (L/T).

Because K_{SG} and K_{LM} characterize relatively small parts of the model domain, it is unlikely that the hydraulic-head and flow data provide enough information to support estimation of these model parameters. Thus, their values are assumed to be known. The value of K_{SG} is fixed at 5×10^{-5} m/s, which is the value used by Rosenberry and Winter (1993) to calculate subsurface seepage from Mirror Lake. The value of K_{LM} is fixed at 1×10^{-9} m/s, which is within the range estimated by Rosenberry and Winter (1993). During model calibration, the values of K_{GD} and K_{BR} are estimated along with recharge from precipitation.

Although parameter structure A offers the appeal of simplicity, it might not adequately represent the hydraulic conductivity in the model domain. To investigate parameter structures of greater complexity, three additional cases are considered. They are referred to as parameter structures B, C, and D (table 5).

Parameter structure B is identical to A except the glacial deposits (excluding sand and gravel south of Mirror Lake) are assumed anisotropic. The components of hydraulic conductivity of glacial deposits in parameter structure B are:

$K_{GD,H}$ = horizontal hydraulic conductivity of glacial deposits, excluding sand and gravel south of Mirror Lake (L/T), and

$K_{GD,V}$ = vertical hydraulic conductivity of glacial deposits, excluding sand and gravel south of Mirror Lake (L/T).

Fine-grained layers in the glacial deposits might impede vertical flow of water, therefore, the vertical hydraulic conductivity is assumed to be less than the horizontal hydraulic conductivity. On the basis of estimates by Rosenberry and Winter (1993), $K_{GD,V}$ is assumed to be one-tenth of $K_{GD,H}$. During model calibration, the value of $K_{GD,H}$ is estimated along with K_{BR} and recharge from precipitation.

Parameter structure C is designed to investigate vertical variability of bedrock hydraulic conductivity. The modeled part of bedrock (uppermost 150 m) is vertically subdivided into three zones corresponding to model layers 3, 4 and 5. The bedrock hydraulic conductivities in parameter structure C are:

$K_{BR,3}$ = hydraulic conductivity of bedrock in model layer 3 (L/T),

$K_{BR,4}$ = hydraulic conductivity of bedrock in model layer 4 (L/T), and

$K_{BR,5}$ = hydraulic conductivity of bedrock in model layer 5 (L/T).

The hydraulic conductivity zonation in model layers 1 and 2 is identical to that of parameter structure A. Isotropy of hydraulic conductivity is assumed in all zones. During model calibration, the values of $K_{BR,3}$, $K_{BR,4}$ and $K_{BR,5}$ are estimated along with K_{GD} and recharge from precipitation.

Parameter structure D is designed to investigate the lateral variability of bedrock hydraulic conductivity. This parameter structure was prompted by data from the newly drilled well FS7 on the ridge at the northwestern corner of the study area (fig. 1). At this well site, the water table was found to be about 15 m below land surface. The shallow water table on the ridge indicates that the water table lies close to land surface over the entire study area. As shown by topographic contours in figure 1, upper hillsides (at altitudes greater than 360 m above sea level) are significantly steeper than lower hillsides (at altitudes less than 360 m above sea level) in the study area. Therefore, the water-table in upper hillsides is expected to be significantly steeper than the water-table in lower hillsides. Using uniform recharge from precipitation and homogeneous hydraulic conductivity in the bedrock, it is not possible to simulate a water

table that has an abrupt change in slope. Therefore, in parameter structure D, the bedrock is laterally subdivided into two zones (fig. 13): (1) a zone beneath upper hillsides and hilltops (stippled), and (2) a zone beneath lower hillsides and valleys (not stippled). In plan view, the boundary separating the two zones approximately coincides with the 360-m contour line. This boundary extends vertically throughout the bedrock (model layers 3, 4 and 5). The bedrock hydraulic conductivities in parameter structure D are:

$K_{BR,U}$ = hydraulic conductivity of bedrock beneath upper hillsides and hilltops(L/T), and

$K_{BR,L}$ = hydraulic conductivity of bedrock beneath lower hillsides and valleys (L/T).

The hydraulic conductivity zonation in model layers 1 and 2 is identical to that of parameter structure A. Isotropy of hydraulic conductivity is assumed in all zones. During model calibration, the values of $K_{BR,U}$ and $K_{BR,L}$ are estimated along with K_{GD} and recharge from precipitation.

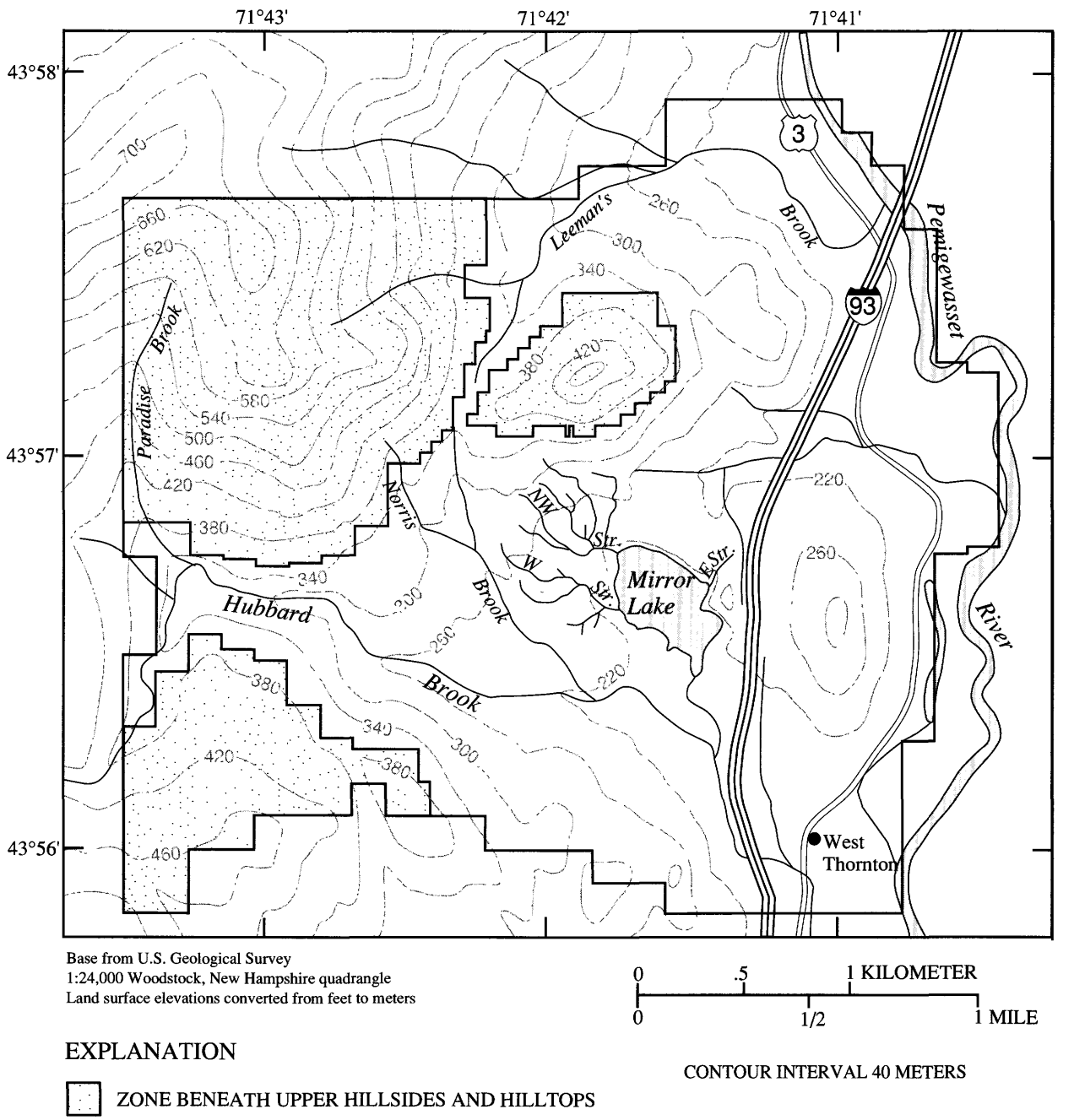

Figure 13. Delineation of the bedrock zone beneath upper hillsides and hilltops used in parameter structure D.

MODEL CALIBRATION

Model calibration (or parameter estimation) is the process of determining unknown model parameters so that simulated quantities match observed quantities (calibration data) to an acceptable level. The parameters determined in this study are (1) rate of recharge from precipitation, (2) hydraulic conductivity of glacial deposits, and (3) hydraulic conductivity of bedrock. Calibration is accomplished by using the computer program MODFLOWP (Hill, 1992), which performs nonlinear least-squares regression. Included in the calibration process is an assessment of parameter uncertainty and goodness of model fit. Calibration is carried out for the four parameter structures A, B, C, and D. These calibrations are referred to as calibrations A, B, C, and D.

CALIBRATION DATA

The two data sets used for model calibration in this study are (1) long-term average baseflow in Streams W, NW, and E at their inlets to Mirror Lake (table 2), and (2) long-term average hydraulic heads measured in piezometers and wells (tables 3 and 4). For brevity, these two data sets are referred to as (1) observed baseflow and (2) observed hydraulic head. Because well FS7 was drilled near the end of this study, when calibrations A, B, and C were already completed, hydraulic head measured in the new well was included only in calibration D.

As noted previously, the measurement location for hydraulic head is taken to be the midpoint of a piezometer screen, or the position of the most transmissive fracture in a well interval. During model calibration, observed hydraulic heads are compared with simulated hydraulic heads at model cells that contain the measurement locations. If two or more measurement locations lie in the same model cell, the observed hydraulic heads are first averaged and then compared with the simulated hydraulic head. If a measurement location lies in a model cell that has become unsaturated during model calibration, the observed hydraulic head is compared with the simulated hydraulic head in the model cell one layer below the unsaturated cell.

NONLINEAR LEAST-SQUARES REGRESSION METHOD

The nonlinear least-squares regression method used for model calibration is based on the formulation of Cooley and Naff (1990). This formulation assumes that a true model exists, and errors (or disturbances) are random, unbiased, and normally distributed (Cooley and Naff, 1990, p. 164–165). In principle, the variance-covariance matrix for the errors can be used to weight the observations. In the present study, this matrix is unknown, and weighting is assigned in a subjective manner on the basis of knowledge of the field data.

Parameters to be estimated (recharge from precipitation and hydraulic conductivities) are denoted by the following notation:

b_i = i^{th} parameter to be estimated,

$\boldsymbol{b}$ = vector of parameters to be estimated,

$\hat{b}_i$ = optimal estimate of the i^{th} parameter, and

$\hat{\boldsymbol{b}}$ = vector of optimal parameters.

In addition,

p = number of parameters to be estimated (dimensionless),

n = total number of observations of hydraulic head and baseflow (dimensionless).

In the actual regression, the common log of hydraulic conductivity is estimated; the result is then exponentiated to yield the estimate for hydraulic conductivity. For example, in calibration A, the parameter vector $\boldsymbol{b}$ consists of $\log(K_{GD})$, $\log(K_{BR})$, and recharge from precipitation. In this case, p equals 3.

The optimal parameters are those that minimize the sum of squared weighted differences between observed and simulated quantities:

$$S(\boldsymbol{b}) = \sum_{i=1}^{n_h} [H_i - h_i(\boldsymbol{b})]^2 + \sum_{i=1}^{n_q} \{w_i^{1/2}[Q_i - q_i(\boldsymbol{b})]\}^2 \quad (4)$$

where

H_i = observed hydraulic head at location i (L),

$h_i(\boldsymbol{b})$ = simulated hydraulic head at location i computed with parameter vector $\boldsymbol{b}$, (L),

n_h = number of hydraulic head observations (dimensionless),

Q_i = observed baseflow in stream i (L^3/T),

$q_i(\boldsymbol{b})$ = simulated baseflow in stream i computed using parameter vector $\boldsymbol{b}$ (L^3/T),
n_q = number of streams (dimensionless), and
$w_i^{1/2}$ = weight on difference between observed and simulated baseflow in stream i (T/L^2).

In calibrations A, B and C, n_h is 90. In calibration D, n_h is 91. The value of n_q is 3 in all cases. The total number of observations, n, is the sum of n_h and n_q.

Because hydraulic head and baseflow are different quantities having different units, weighting is necessary to combine both into a single optimization criterion (equation 4). For Streams W and NW, the weights are chosen such that a 1 percent difference between observed and simulated baseflow is equivalent to a 1 m difference between observed and simulated hydraulic head. For Stream E, the weight is such that a 5 percent difference between observed and simulated baseflow is equivalent to a 1 m difference between observed and simulated hydraulic head. The unequal weighting is appropriate because Stream E drains a much smaller sub-basin than Streams W or NW, and therefore exerts a much smaller influence on the overall ground-water system. The unequal weighting allows a larger tolerance when matching observed and simulated baseflow to the E Stream than to Streams W and NW.

The minimization of $S(\boldsymbol{b})$ is accomplished with the computer program MODFLOWP (Hill, 1992), which uses a modified Gauss-Newton method to determine the optimal MODFLOW parameters. As noted previously, the model in this study requires that at each cell in the horizontal dimension, the computed water table be allowed to lie in any of the five model layers. Consequently, the saturated thickness of each model layer is determined during the model simulation. However, the version of MODFLOWP used in this study does not allow the water-table position to vary during a model simulation, and thus requires that the saturated thickness of each layer be specified. To overcome this problem, an iterative scheme is used. Starting with a set of assumed parameters, MODFLOW is executed, the water table position is computed during the simulation, and saturated thicknesses are computed and stored. Next, a MODFLOWP calibration is run with the saturated thicknesses set equal to those obtained from the prior MODFLOW simulation. If the parameters estimated by MODFLOWP differ significantly from those used in MODFLOW, the procedure is repeated. In the next iteration, parameters estimated by MODFLOWP are used in MODFLOW to obtain new saturated thicknesses. The new saturated thicknesses are then used in MODFLOWP to obtain new parameter estimates. This iterative process continues until the parameter estimates no longer change from one iteration to the next.

OPTIMAL ESTIMATES OF RECHARGE FROM PRECIPITATION AND HYDRAULIC CONDUCTIVITY

Examination of the results of model calibration (table 6) shows that, for many model parameters, the four calibrations A, B, C, and D yield optimal estimates that are similar to each other. The four optimal estimates of recharge from precipitation all fall within a narrow range from 26 to 28 cm/year.

Table 6. Optimal estimates of recharge from precipitation and hydraulic conductivities.

[Recharge in centimeters per year; hydraulic conductivity in meters per second; --, not used in parameter structure]

Parameter	Optimal estimate in calibration			
	A	B	C	D
Recharge from precipitation	27	26	27	28
K_{GD}	2.67×10^{-6}	--	2.54×10^{-6}	1.74×10^{-6}
$K_{GD,H}$	--	2.57×10^{-6}	--	--
$K_{GD,V}$[1]	--	2.57×10^{-7}	--	--
K_{BR}	2.93×10^{-7}	3.05×10^{-7}	--	--
$K_{BR,3}$	--	--	3.10×10^{-7}	--
$K_{BR,4}$	--	--	2.89×10^{-7}	--
$K_{BR,5}$	--	--	2.78×10^{-7}	--
$K_{BR,U}$	--	--	--	6.26×10^{-8}
$K_{BR,L}$	--	--	--	3.21×10^{-7}

[1] In parameter structure B, $K_{GD,V}$ is preset to equal one-tenth of $K_{GD,H}$.

These values represent approximately 20 percent of the long-term average precipitation measured at the Forest Service station and are near the lower limit of the range (16 to 45 percent) estimated by Mau and Winter (1997).

In the parameter structures where glacial deposits are assumed isotropic (calibrations A, C and D), the optimal estimates of K_{GD} are also similar to each other, ranging from 1.7×10^{-6} to 2.7×10^{-6} m/s. These values lie between the slug-test estimates for till and for sand and gravel as determined by Winter and Rosenberry (table 1). If glacial deposits are assumed anisotropic (calibration B), the optimal estimate of $K_{GD,H}$ is similar to those of K_{GD}. The value of $K_{GD,V}$ was preset to equal one-tenth of $K_{GD,H}$.

Optimal estimates of bedrock hydraulic conductivity also show similarities. In the parameter structures where the bedrock is assumed uniform (calibrations A and B), the optimal estimates of K_{BR} are both about 3×10^{-7} m/s. This value is consistent with the effective hydraulic conductivity of 2×10^{-7} m/s determined by Hsieh and Shapiro (1994) for the bedrock underlying the FSE well field. If the bedrock is vertically subdivided by model layers (calibration C), the optimal estimates of $K_{BR,3}$, $K_{BR,4}$ and $K_{BR,5}$ are all about 3×10^{-7} m/s. The absence of a significant trend in these values indicates that the calibration data in the present study do not support the hypothesis that hydraulic conductivity varies with depth in the modeled part (uppermost 150 m) of bedrock. If the bedrock is laterally subdivided according to land-surface altitude (calibration D), the optimal estimate of $K_{BR,L}$ is similar to those of K_{BR}, but the optimal estimate of $K_{BR,U}$ is about one-fifth of $K_{BR,L}$. These results indicate that 3×10^{-7} m/s is a reasonable hydraulic conductivity for bedrock beneath lower hillsides and valleys, but a lesser value (6×10^{-8} m/s) might be more appropriate for bedrock beneath upper hillsides and hilltops. However, because the estimation of $K_{BR,U}$ is based largely on the single hydraulic head measured at the newly drilled well FS7, additional data are required to further confirm this result.

PARAMETER UNCERTAINTY

Within the context of regression analysis, parameter uncertainty can be assessed by calculating a confidence interval for each parameter. These confidence intervals should be interpreted with caution, because they are computed under the assumption that errors can be approximated by residuals (differences between observed and simulated quantities). In this approach, model attributes such as geometry, zonation, boundary conditions, and values of non-estimated parameters (table 5) are assumed perfectly known. Errors or uncertainties in these model attributes could greatly increase the uncertainty of estimated parameters.

The confidence intervals computed in this study are known as approximate, individual confidence intervals. The intervals are approximate because the computation assumes that the model is effectively linear in the vicinity of the optimal parameters. The intervals are individual in that they are computed for each parameter while holding all other parameters at their optimal values. In addition, the computation assumes that errors are independent and normally distributed. Because the above assumptions might not be satisfied in calibrations of the ground-water model for this study, their validity is examined.

To calculate confidence intervals, it is necessary to first calculate the variance-covariance matrix for the parameters, which is (Cooley and Naff, 1990, p. 167, eq. 5.4–13)

$$\boldsymbol{V}(\hat{\boldsymbol{b}}) = s^2 (\boldsymbol{X}^T \omega \boldsymbol{X})^{-1} , \qquad (5)$$

where s^2 is defined as (Cooley and Naff, 1990, p. 166, eq. 5.4–5)

$$s^2 = \frac{S(\hat{\boldsymbol{b}})}{n-p} , \qquad (6)$$

where $S(\hat{\boldsymbol{b}})$ is computed using equation 4 and the optimal parameters $\hat{\boldsymbol{b}}$, ω is the n by n diagonal matrix of weights (which equals one for hydraulic heads and $w_i^{1/2}$ for baseflow in stream i), and $\boldsymbol{X}$ is the n by p sensitivity matrix containing derivatives of simulated hydraulic head or baseflow at the measurement locations with respect to model parameters $\boldsymbol{b}$, evaluated at the optimal parameters $\hat{\boldsymbol{b}}$. The i^{th} element on the main diagonal of $\boldsymbol{V}(\hat{\boldsymbol{b}})$ is the variance, V_{ii}, for the i^{th} parameter. After the variance-covariance matrix is computed, the approximate, individual, 100(1-α) percent confidence interval for the i^{th} parameter is given by (Hill, 1992, page 58)

$$\hat{b}_i \pm V_{ii}^{1/2} \times t\left(n-p, 1-\frac{\alpha}{2}\right), \quad (7)$$

where $t(n\text{-}p,1\text{-}a/2)$ is the $100(1\text{-}a/2)$ percentage point of the Student-t distribution with $n\text{-}p$ degrees of freedom.

The approximate, individual, 95-percent confidence intervals for recharge from precipitation and hydraulic conductivities are shown in figure 14. In all four calibrations, the confidence intervals for recharge span approximately the same width—about 15 percent of the optimal estimate—indicating that the four recharge estimates have similar levels of uncertainty. For hydraulic conductivities, confidence intervals in calibrations A, B and D are much narrower than those in calibration C. This comparison indicates that hydraulic conductivity estimates are much better constrained in calibrations A, B and D, but they are subject to much greater uncertainty in calibration C. The relatively high uncertainty in calibration C is an additional indication that the calibration data do not support the hypothesis that hydraulic conductivity varies with depth in the modeled portion (uppermost 150 m) of bedrock.

Because the confidence intervals in figure 14 are computed under the assumptions that (1) the model is effectively linear about the optimal parameters and (2) errors are independent and normally distributed, the validity of these assumptions should be examined. In this study, the degree of model nonlinearity is examined by the "modified Beale's measure" (Cooley and Naff, 1990, p. 187). Independence and normality of errors are inferred from analysis of weighted residuals, which are weighted differences between observed and simulated quantities (hydraulic heads and baseflows).

Modified Beale's measures calculated by the computer program BEALEP (Hill, 1994, p. 45–54) are shown in table 7. On the basis of criteria suggested by Cooley and Naff (1990, p. 189), these modified Beale's measures are interpreted as follows: the model is effectively linear if the modified Beale's measure is less than 0.03; the model is highly nonlinear if the modified Beale's measure is greater than 0.37. In calibrations A, B, and D, the modified Beale's measure lies between 0.03 and 0.37, indicating that although the model is nonlinear, it is not highly nonlinear. In calibration C, the modified Beale's

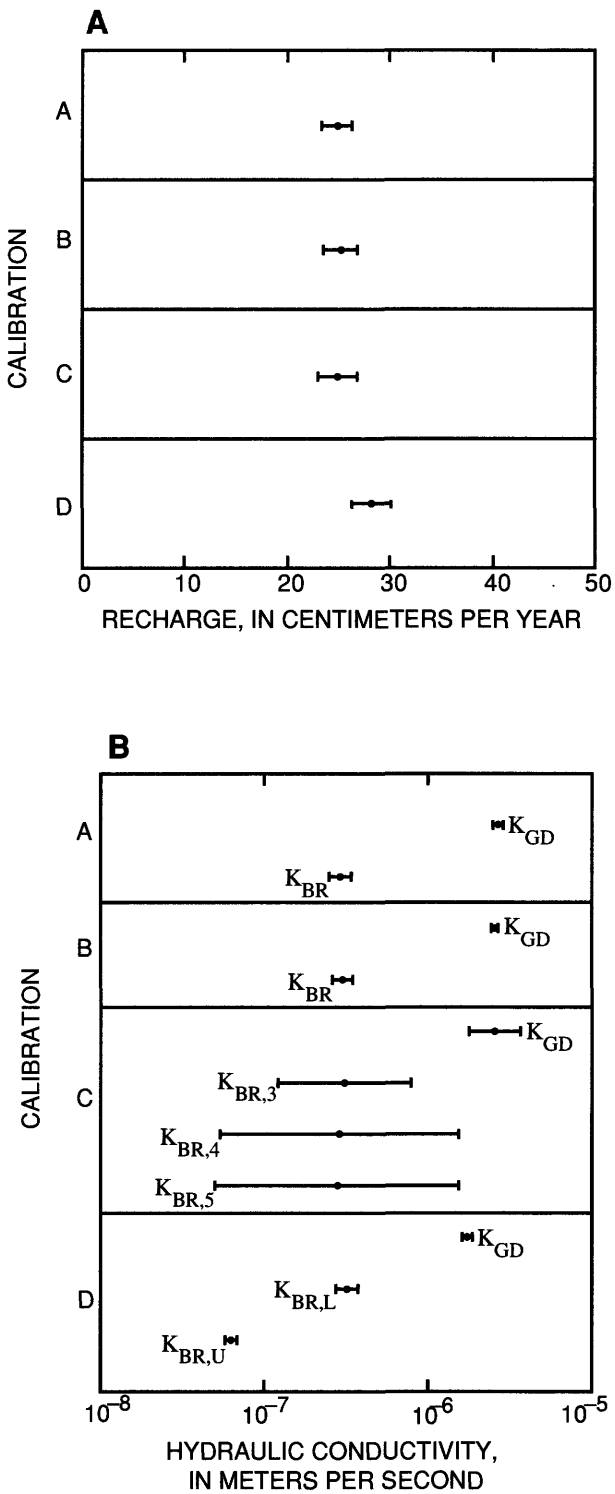

Figure 14. Approximate, individual, 95-percent confidence intervals for (A) recharge from precipitation and (B) hydraulic conductivities.

measure is significantly larger than 0.37, indicating a high degree of nonlinearity.

Table 7. Modified Beale's measure, R_N^2, and critical value of R_N^2.
[All statistics dimensionless]

Statistic	Value in calibration			
	A	B	C	D
Modified Beale's measure	0.14	0.22	21.7	0.26
R_N^2	0.925	0.919	0.943	0.899
Critical value of R_N^2	0.973	0.973	0.973	0.974

In the analysis of weighted residuals, the residual for hydraulic head is assigned a weight of unity, and the residual for baseflow in stream i is assigned the weight $w_i^{1/2}$. To examine normality, weighted residuals for each parameter structure are plotted on normal probability plots (fig. 15). For parameter structures A and C, the weighted residuals form a nearly straight line on the normal probability plots. The plots for parameter structures B and D each contain one weighted baseflow residual that is an outlier, but the remainder of the weighted residuals for these two parameter structures plot nearly on a straight line. Therefore, the normal probability plots indicate that the distribution of weighted residuals for all the parameter structures is close to normal. To examine both normality and independence, a hypothesis test suggested by Hill (1992, p. 63) is used. This test is based on the correlation coefficient (denoted by R_N^2) between the weighted residuals ordered from smallest to largest and the order statistics from the normal probability distribution function. If the R_N^2 falls below a critical value (given by Hill, 1992, p. 64) the hypothesis that the weighted residuals are independent and normally distributed is rejected. Table 7 shows that for all four parameter structures, R_N^2 lies close to, but nonetheless falls below, the critical value. Therefore, strictly speaking, the hypothesis of independence and normality is rejected. However, if the normal probability plots (fig. 15) are considered together with the hypothesis test, the overall results indicate that the weighted residuals (and by inference, the errors) might be close to independent and normally distributed.

The above analyses of the modified Beale's measure and weighted residuals indicate that the assumptions of linearity, independence, and normality are not strictly valid. Nonetheless, in calibrations A, B, and D, these assumptions appear nearly satisfied. Thus the computed confidence intervals could be considered rough indicators of parameter uncertainty. In calibration C, the linearity assumption appears seriously incorrect. Thus, the computed confidence intervals could be subject to large inaccuracies.

GOODNESS OF MODEL FIT

The overall goodness of model fit can be assessed by examining statistics of residuals (observed values minus simulated values). In general, a lower residual statistic indicates a better overall model fit. The sum of squared weighted residuals, $S(\hat{\boldsymbol{b}})$, defined by equation 4 with $\hat{\boldsymbol{b}}$ being the vector of optimal parameters, gives an overall measure of model fit to all observations. In addition, the sum of squared residuals of hydraulic head, defined as

$$S_h = \sum_{i=1}^{n_h} \left[H_i - h_i(\hat{\boldsymbol{b}})\right]^2, \tag{8}$$

gives an overall measure of model fit to hydraulic head. The sum of squared weighted residuals of baseflow, defined as

$$S_q = \sum_{i=1}^{n_q} \left\{w_i^{1/2}\left[Q_i - q_i(\hat{\boldsymbol{b}})\right]\right\}^2. \tag{9}$$

gives an overall measure of model fit to baseflow. Finally, the standard error of hydraulic head, defined as

$$s_h = \left(\frac{S_h}{n_h - p}\right)^{1/2} \tag{10}$$

gives the average (root-mean-square) discrepancy between observed and simulated hydraulic heads. The standard error of baseflow cannot be calculated because of insufficient data for statistical analysis.

Computed values of residual statistics for calibrations A through D, and the maximum and minimum residual of hydraulic head in each calibra-

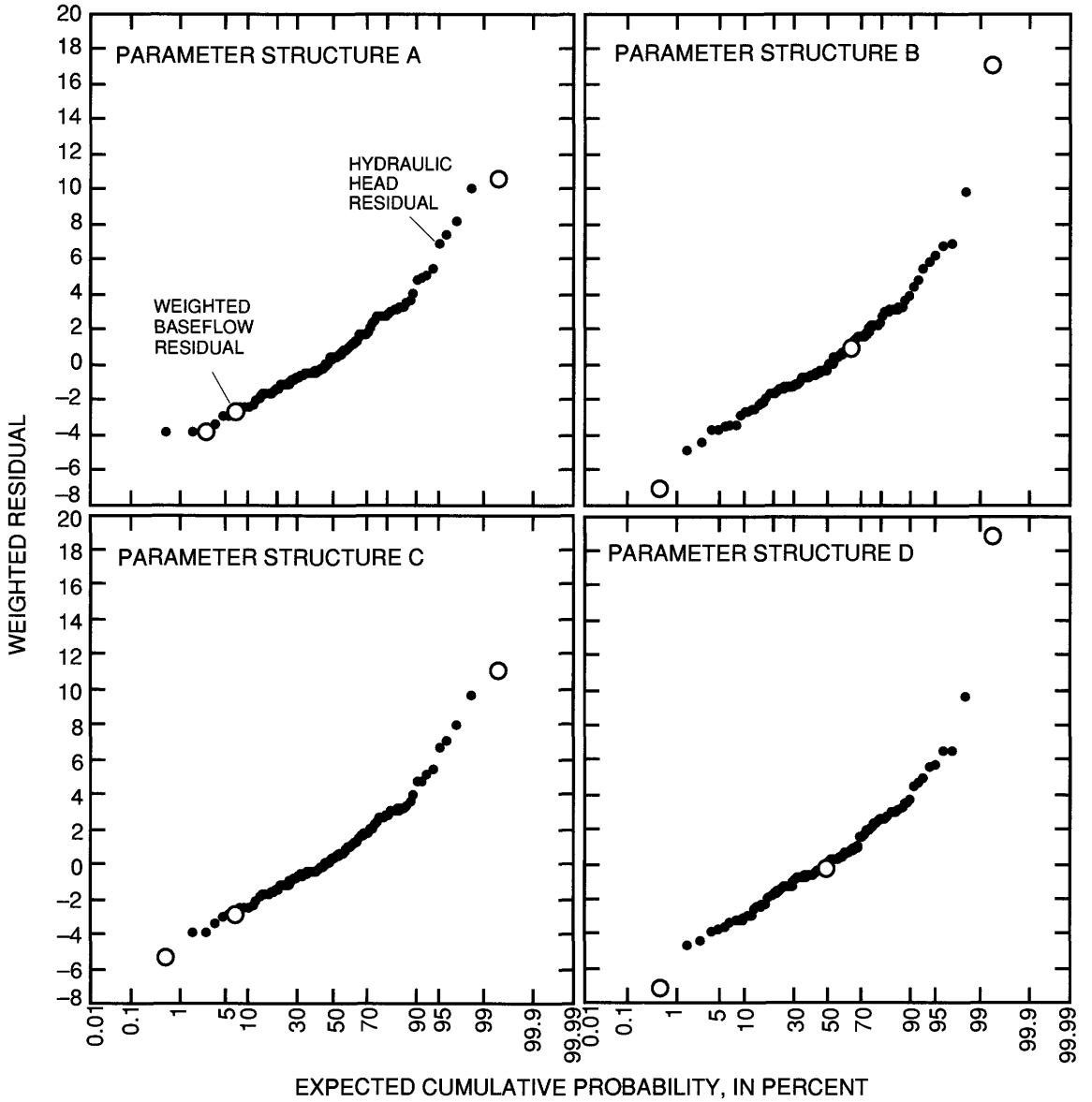

Figure 15. Normal probability plots of weighted residuals.

tion are given in table 8. Because calibration D includes an extra hydraulic head measured at the newly drilled well FS7, it is considered separately from the other three calibrations. Comparison of residual statistics for calibrations A, B, and C shows that $S(\hat{b})$ is highest in B, and is the same in A and C. The poorer fit in calibration B is due to a poorer fit to baseflow. The fit to hydraulic head is about the same in all three calibrations. The standard error of hydraulic head in all three cases is about 2.8 m, which is relatively small compared with the 145 m of elevation difference between the highest and lowest observed hydraulic head. Observed and simulated baseflow differ by less than 10 percent in Streams W and NW (table 9), which together account for more than 90 percent of total baseflow. These results lead to two conclusions. First, calibrations A, B, and C all yield relatively good overall model fits. Second, the model fit in calibration A is not improved by introducing a 10-to-1 ratio of horizontal-to-vertical anisotropy in hydraulic conductivity of glacial deposits (calibration B), or by varying hydraulic conductivity with depth in the modeled part (uppermost 150 m) of the bedrock (calibration C).

Table 8. Residual statistics used to measure overall goodness of model fit.

[Sum of squared weighted residuals and sum of squared residuals in square meters; standard error, maximum residual and minimum residual of hydraulic head in meters]

Statistic	Value in calibration			
	A[1]	B[1]	C[1]	D[2]
Sum of squared weighted residuals, $S(\hat{b})$	799	1017	799	1048
Sum of squared residuals of hydraulic head, S_h	665	677	641	636
Sum of squared weighted residuals of baseflow, S_q	134	340	158	412
Standard error of hydraulic head, s_h	2.76	2.79	2.75	2.70
Minimum residual of hydraulic head[3]	-4.0	-4.9	-3.9	-4.7
Maximum residual of hydraulic head[3]	10.0	9.8	9.7	9.5

[1]does not include hydraulic-head residual at well FS7.
[2]includes hydraulic-head residual at well FS7.
[3]Positive residual indicates that observed value is higher than simulated value. Negative residual indicates that observed value is lower than simulated value.

Table 9. Observed and simulated baseflow in Streams W, NW, and E.

[Baseflow in cubic meters per year]

Stream	Observed baseflow	Baseflow simulation with parameter structure			
		A	B	C	D
W	63,000	60,200	63,500	59,500	62,800
NW	100,000	97,100	92,300	96,700	92,300
E	5,000	7,300	8,800	7,300	9,200
Total	168,000	164,600	164,600	163,500	164,300

If taken at face value, the residual statistics for calibration D show that the overall model fit in calibration D is no better (in fact, a bit worse) than the overall model fit in calibration A. Such an assessment is correct as long as it is confined to lower hillsides and valleys, that is, the region in which hydraulic heads are measured for calibration A. However, calibration D includes an extra hydraulic-head measured at the newly drilled well FS7, located near the highest point of the study area. The simulated hydraulic head at FS7 is within 1 m of the observed hydraulic head. In this regard, calibration D yields a more realistic simulation than calibration A at higher altitudes. This conclusion, however, should be considered preliminary and requires further confirmation using additional observations of hydraulic heads at higher altitudes.

In addition to an overall assessment of model fit, a more detailed assessment can be made by examining the spatial distribution of hydraulic-head residuals. Figure 16 shows this distribution in the five model layers over an area in which most of the piezometer and wells are located. Residuals are shown only for calibration A, because similar results are obtained for the other three calibrations. Although most of the residuals in figure 16 are relatively small (many fall within the range from -4 m to 4 m), their spatial distribution in model layers 1 and 2 (glacial deposits) shows an obvious pattern. In these two layers, residuals in the area northwest of Mirror Lake are generally positive (observed values higher than simulated values), and residuals in the area south of Mirror Lake are generally negative (observed values lower than simulated values). This pattern suggests that residuals in layers 1 and 2 are not random, but that they exhibit trends due to limitations imposed by model assumptions of uniform recharge from precipitation and

homogeneous hydraulic conductivity in each hydrogeologic unit. Each of model layers 3, 4, and 5 contains too few residuals to draw inferences about their spatial distribution.

The lack of fit between simulated and observed hydraulic heads at the local scale is further illustrated in figure 17, which shows hydraulic-head contours in the vertical section AB (see fig. 8) on a hillside west of Mirror Lake. In general, simulated contours match observed contours in conveying the sense of lateral ground-water flow in the downslope direction. However, detailed examination of the two sets of contours shows distinct differences. The observed contours have an irregular pattern, suggesting that flow is locally affected by nonuniform recharge and/or heterogeneous hydraulic conductivity. The simulated contours have a more regular pattern, because of the model assumptions of uniform recharge and homogeneous hydraulic conductivity. This comparison further shows that the model developed in this study characterizes the generalized ground-water flow system, not local details.

SIMULATION OF GROUND-WATER FLOW

The major objective of simulating ground-water flow in the Mirror Lake area is to determine the three-dimensional extent of the Mirror Lake ground-water basin and the ground-water budget for the basin. Because four parameter structures are used in model calibration, four sets of simulation results are obtained. In this study, it is found that simulations using parameter structures A, B, and C yield similar results. Therefore, only simulations using parameter structures A and D are presented. These two simulations are referred to as simulation A and simulation D. Although simulation D is expected to be more realistic than simulation A at higher altitudes of the Mirror Lake area, both simulations are presented for comparison.

WATER TABLE

The water-table configuration for simulation A is shown in figure 18, and that for simulation D is shown in figure 19. The two water-table configurations are similar at lower altitudes, but differ significantly at upper altitudes. At the northwestern corner of the model domain, the water table in simulation A rises to 560 m above sea level (about 100 m below land surface), whereas the water table in simulation D rises to 640 m above sea level (about 20 m below land surface). The shallower water table in simulation D results from using a lower hydraulic conductivity for bedrock beneath upper hillsides in order to match the newly observed hydraulic head at well FS7. This new observation was not used in the calibration process for simulation A.

Areas where the simulated water table lies in the glacial deposits are also shown in figures 18 and 19. In these areas, recharge from precipitation enters the glacial deposits. Outside these areas, the simulated water table lies in the bedrock, and recharge from precipitation enters the bedrock, either by infiltration through the overlying unsaturated glacial deposits, or directly from land surface where bedrock crops out. Areas where the glacial deposits are absent or unsaturated occur mostly on upper hillsides and away from streams. Because the water table is deeper in simulation A than in simulation D, unsaturated glacial deposits cover a larger area in simulation A. Consequently, more of the water table lies in bedrock in simulation A than in simulation D, and therefore more recharge from precipitation enters the bedrock in simulation A than in simulation D. Conversely, less recharge from precipitation enters the glacial deposits in simulation A than in simulation D.

MIRROR LAKE GROUND-WATER BASIN

The Mirror Lake ground-water basin refers to the volume of subsurface through which ground water flows from the water table to Mirror Lake or its three inflow streams. The three-dimensional extent of the basin is determined by tracking ground-water flow paths in a reverse direction from Mirror Lake and its inflow streams back to the water table. The volume spanned by these flow paths delineates the Mirror Lake ground-water basin. In this study, flow paths are computed with the computer program MODPATH (Pollock, 1994), a particle tracking post-processor package for MODFLOW.

In the MODPATH simulations, the starting positions of particles are chosen so that ground-water flow paths entering the sides and bottom of Mirror

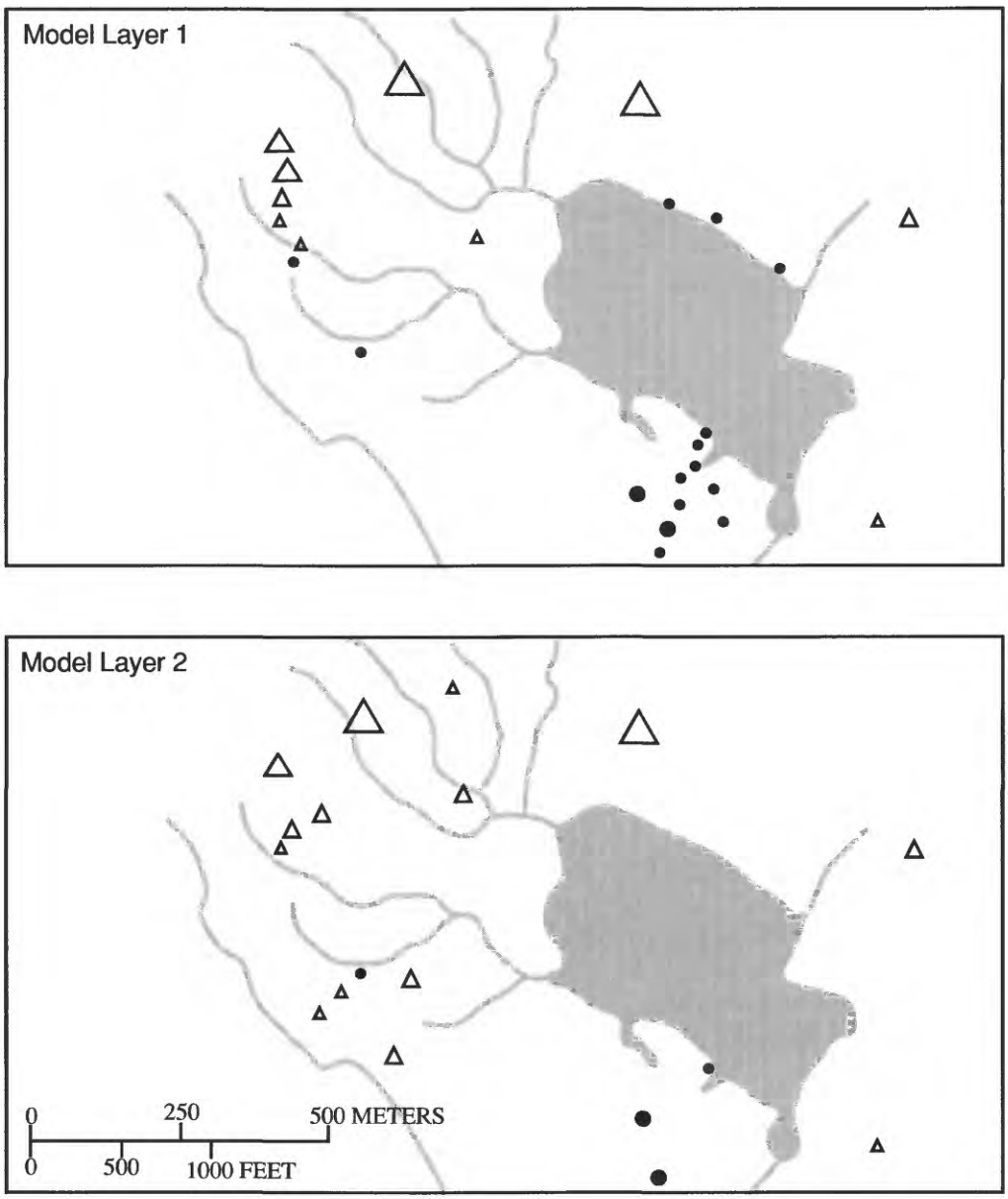

Figure 16. Distribution of hydraulic head residuals in model layers 1 through 5 in calibration A.

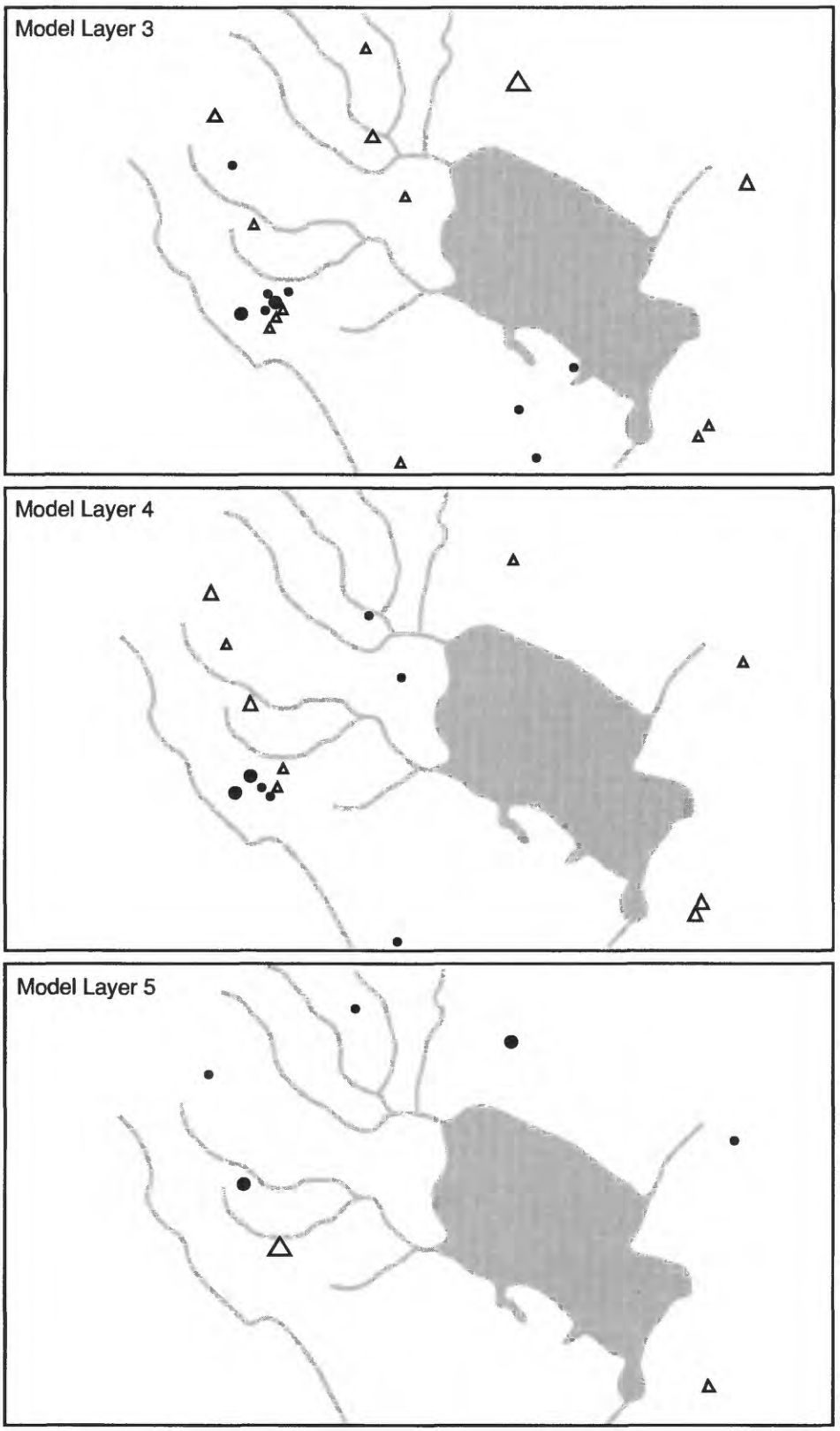
Model Layer 3
Model Layer 4
Model Layer 5

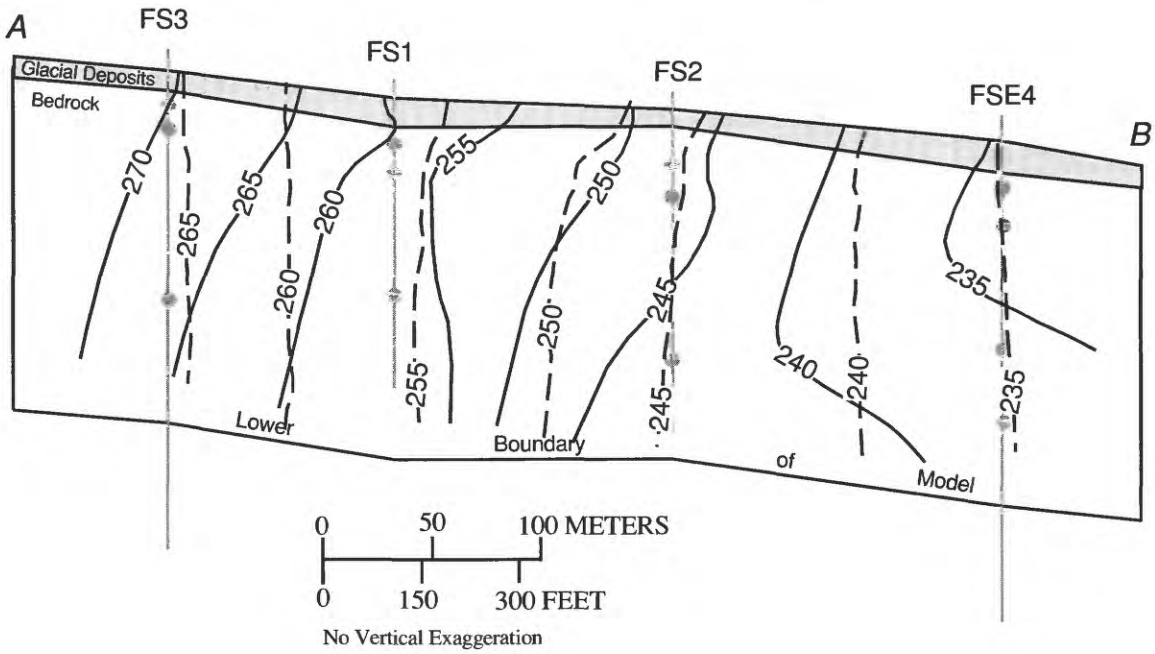

EXPLANATION

—240— OBSERVED HYDRAULIC-HEAD CONTOUR-Contour interval 5 meters. Datum is sea level.

– – 240– HYDRAULIC-HEAD CONTOUR SIMULATED WITH PARAMETER STRUCTURE A-Contour interval 5 meters. Datum is sea level.

● HYDRAULIC-HEAD MEASUREMENT LOCATION-Shows location of the highest-transmissivity fracture in a well interval.

Figure 17. Observed and simulated hydraulic head in section A-B. (See figure 8 for location of line of section.)

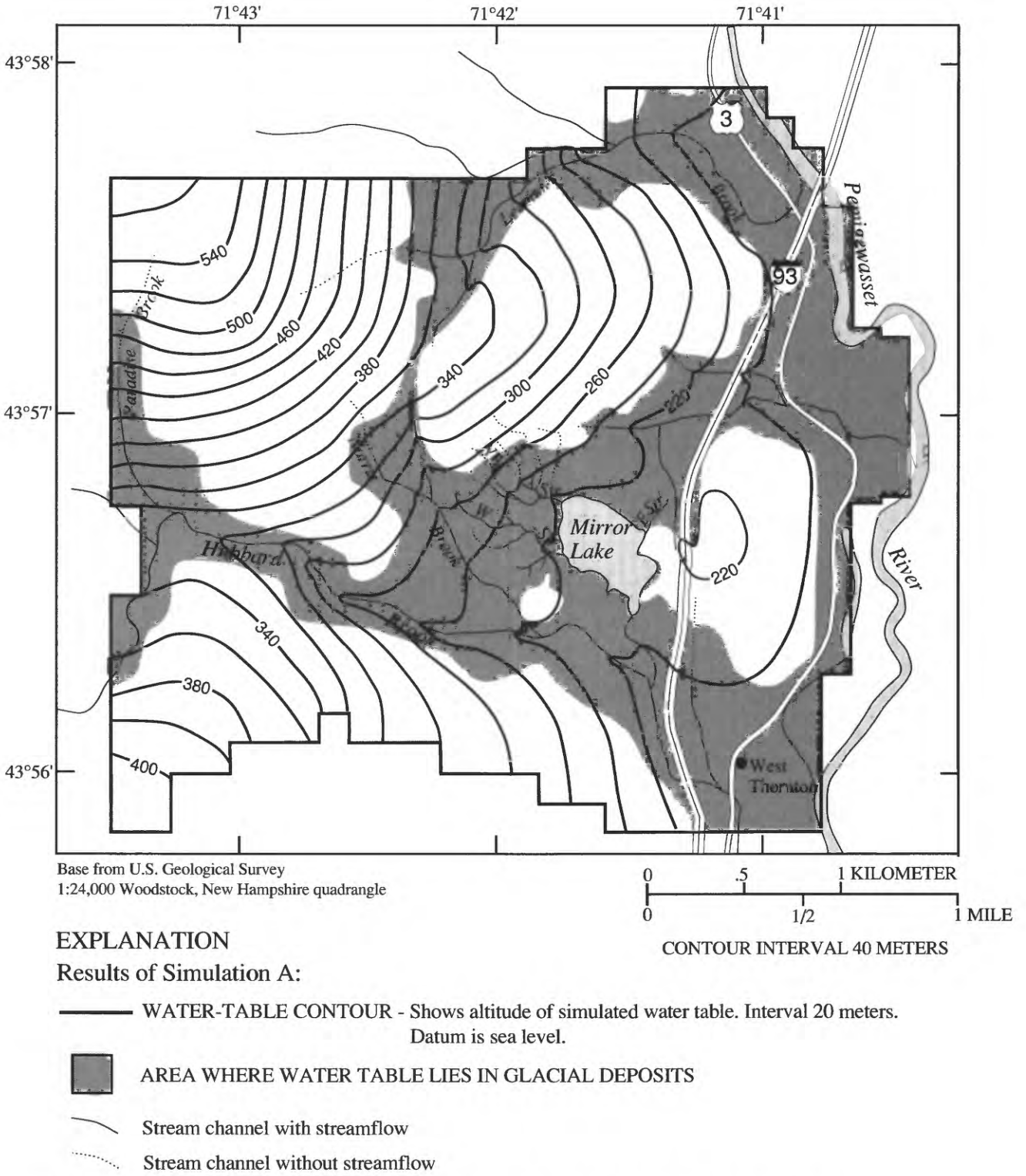

Figure 18. Water table for simulation A, and areas where water table lies in glacial deposits.

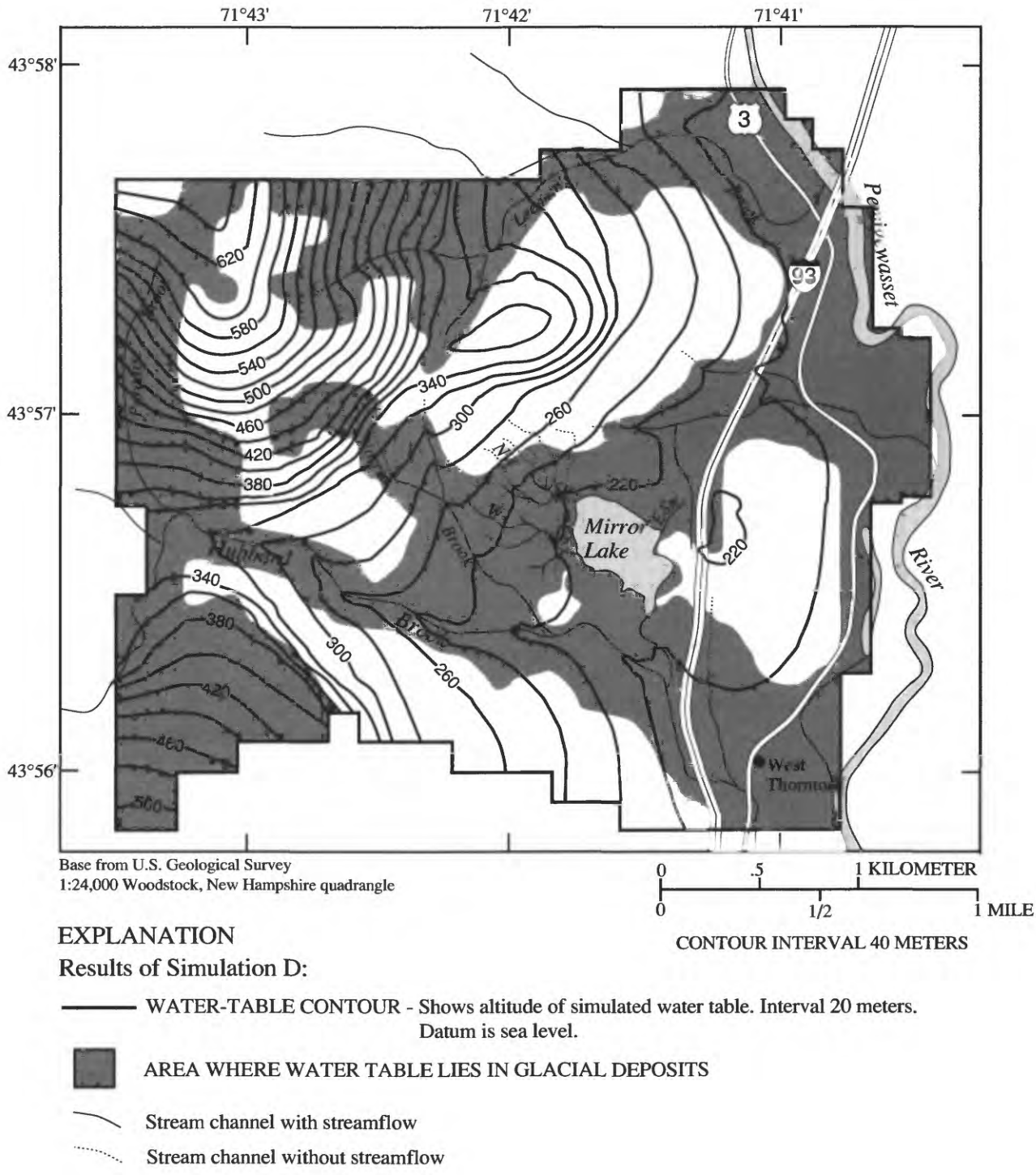

Figure 19. Water table for simulation D, and areas where water table lies in glacial deposits.

Lake and its inlet streams are tracked backwards. Twenty-five particles are placed in each finite-difference cell representing Mirror Lake and in each cell containing a reach of Stream W, NW, or E. Five particles are placed on each side face and on the bottom face of these cells. One particle is placed in the center of the face, and one is placed near each corner of the face.

The horizontal extent of the Mirror Lake ground-water basin for simulation A is shown in figure 20, and the three-dimensional extent is shown in figure 21. Corresponding illustrations for simulation D are shown in figures 22 and 23. In both simulations, the ground-water basin extends far up the hillside in the northwestern part of the study area (fig. 20 and 22), and ground water flows across the topographic divide that forms the northwestern boundary of the surface-water basin. At the southern end of Mirror Lake, the area of subsurface seepage from the lake is not included in the Mirror Lake ground-water basin because ground water in this area flows towards Hubbard Brook.

In figures 20 and 22, the horizontal extent of the Mirror Lake ground-water basin is divided into a "recharge zone" (heavily shaded area) and two "underflow zones" (lightly shaded areas). The recharge zone is an area where the top of the ground-water basin is coincident with the water table. Recharge entering this area eventually drains to Mirror Lake or its inlet streams. In both simulations A and D, the size of the recharge zone is about 1.5 times the size of the surface-water basin. In other words, the area from which ground-water recharge drains to Mirror Lake or its inlet streams is about 1.5 times the area of surface-water drainage to the lake. The underflow zones shown on figures 20 and 22 are areas where the top of the ground-water basin lies below the water table. In these areas, the Mirror Lake ground-water basin lies beneath overlying ground-water basins.

In figures 21 and 23, the heavily shaded surface on the three-dimensional rendering of the ground-water basin is the water table. This surface corresponds to the heavily shaded area (recharge zone) on the overlying map. Flow paths in both simulations A and D show that a portion of recharge occurring on the northwestern part of the recharge zone flows at depth under Norris Brook to discharge into Mirror Lake or its inlet streams. In the shallow saturated zone around Norris Brook, recharge to the water table flows to Norris Brook to form a separate ground-water basin. Therefore, part of the Mirror Lake ground-water basin lies beneath the adjacent ground-water basin that drains into Norris Brook. The lightly shaded surface on figures 21 and 23 is the boundary below the water table that separates the Mirror Lake ground-water basin and the overlying Norris Brook ground-water basin. No flow occurs across this surface. Below this surface, ground water flows to Mirror Lake and its inlet streams. Above this surface, ground water flows to Norris Brook. The horizontal extent of this surface corresponds to the larger of the two lightly shaded areas (underflow zones) on the overlying map. A smaller underflow zone occurs on the north side of the basin in each simulation (fig. 20 and 22). The surface corresponding to this underflow zone is hidden from view in figures 21 and 23.

Two sets of additional MODPATH simulations are performed to examine the sensitivity of the position and extent of the Mirror Lake ground-water basin to variations in initial particle placement. First, the number of particles placed on the faces of cells containing Mirror Lake and Streams W, NW, and E is reduced, and second, particles are placed in a lattice arrangement within the cells instead of on the cell faces. In these simulations, the location and size of the Mirror Lake ground-water basin do not significantly differ from the location and size of the basin delineated in the simulation with five particles on each of the bottom and side faces.

GROUND-WATER BUDGET

The ground-water budget for the Mirror Lake ground-water basin gives an accounting of recharge to the basin, discharge from the basin, and flow between hydrogeologic units in the basin. These budget components are illustrated in figure 24. Recharge to the ground-water basin includes:

R_1 = recharge from precipitation to bedrock (L^3/T),

R_2 = recharge from precipitation to glacial deposits (L^3/T), and

R_3 = recharge from streams to glacial deposits (L^3/T), which occurs along losing reaches of Streams W and NW.

Discharge from the ground-water basin includes:

D_1 = discharge from glacial deposits to streams (L^3/T),

D_2 = discharge from glacial deposits to Mirror Lake (L^3/T),

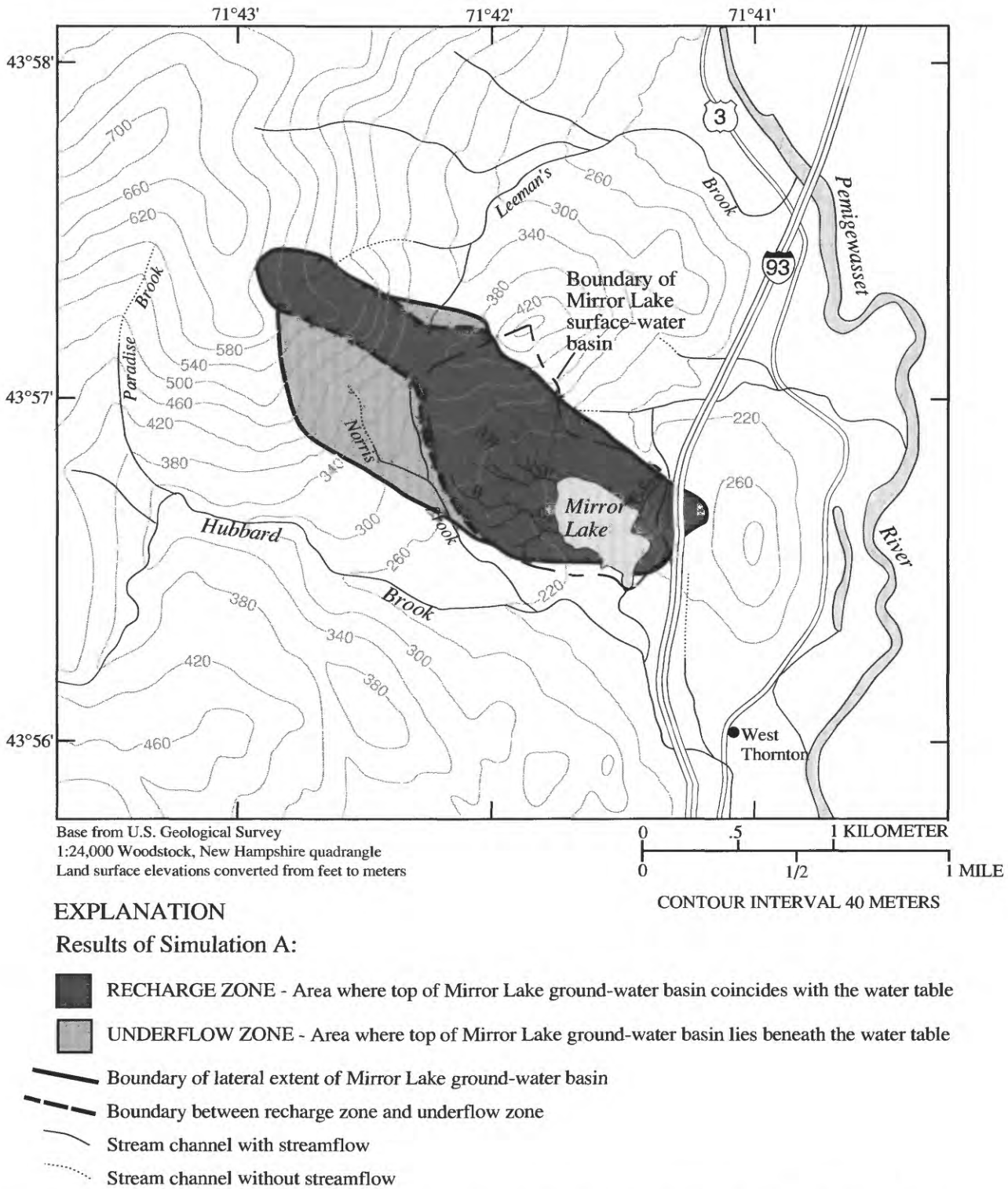

Figure 20. Horizontal extent of Mirror Lake ground-water basin in simulation A. Mirror Lake surface-water basin is included for comparison.

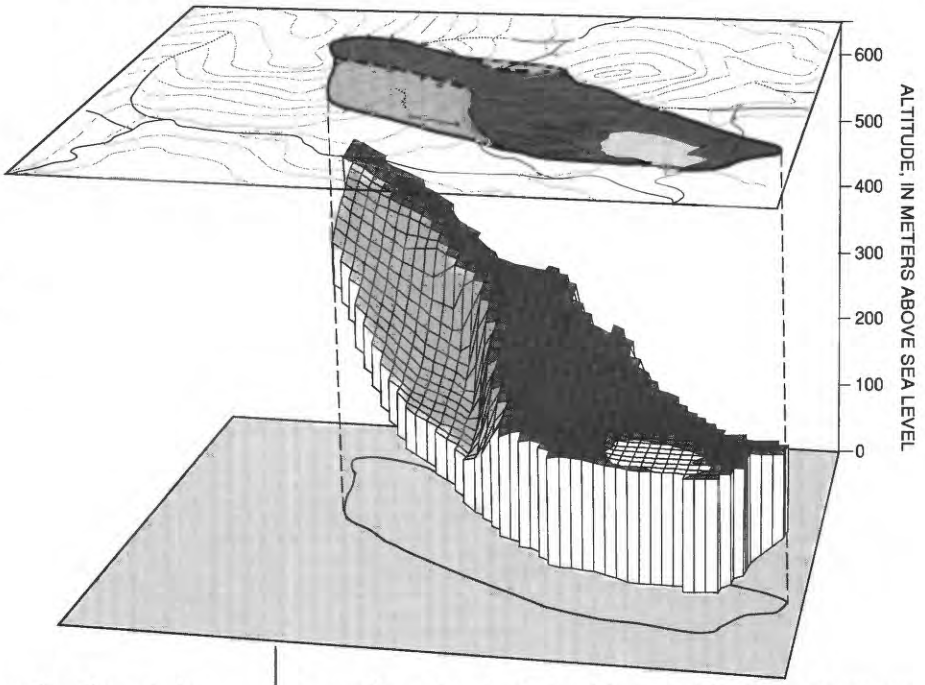

Figure 21. Three-dimensional extent of Mirror Lake ground-water basin in simulation A. See figure 20 for explanation.

D_3 = discharge from lacustrine mud sediments to Mirror Lake (L^3/T), and

D_4 = discharge from bedrock to Mirror Lake (L^3/T), which occurs where bedrock crops out on the east side of the lake

Flow between hydrogeologic units in the ground-water basin includes

B_1 = flow from glacial deposits to bedrock (L^3/T),

B_2 = flow from bedrock to glacial deposits (L^3/T), and

B_3 = flow from bedrock to lacustrine mud sediments (L^3/T).

Under steady state, total recharge to the ground-water basin, defined as

$$R_T = R_1 + R_2 + R_3 \qquad (11)$$

equals total discharge from the basin, defined as

$$D_T = D_1 + D_2 + D_3 + D_4 \,. \qquad (12)$$

Budget components are computed by the computer program ZONEBUDGET (Harbaugh, 1990), which calculates subregional water budgets using simulation results from MODFLOW. Results are given in table 10.

In both simulations A and D, computed total recharge to the Mirror Lake ground-water basin (R_T) is approximately 300,000 m^3/year. Nearly all the recharge is derived from precipitation ($R_1 + R_2$); only a small portion is derived from infiltration of stream water along losing reaches of streams (R_3). The recharge from precipitation enters the basin either in areas where the simulated water table lies in the bedrock (R_1) or in areas where the simulated water table lies in the glacial deposits (R_2). Although in simulation A the amount of recharge entering the bedrock is slightly greater than that entering the glacial deposits, in both simulations A and D roughly half of the recharge enters each of the two hydrogeologic units.

Of the total discharge from the Mirror Lake ground-water basin (D_T), in both simulations A and D slightly more than half flows into Streams W, NW and E (D_1), slightly less than half flows into Mirror Lake from the glacial deposits (D_2), and minute amounts enter Mirror Lake from the lacustrine mud (D_3) and from the bedrock where it crops out on the east side of the lake (D_4). In both simulations A and D, computed total ground-water seepage to Mirror Lake ($D_2 + D_3 + D_4$) is approximately 130,000 m^3/year. Although this value is greater than Rosenberry and Winter's (1993) estimate of 80,000 m^3/year, it is within the range of uncertainty (±100 percent) for their estimate.

Within the Mirror Lake ground-water basin, flows between hydrogeologic units are strongly controlled by the direction of the vertical flow component. Flow from glacial deposits to bedrock (B_1) occurs primarily beneath upper hillsides, where the vertical component of flow is predominantly downward. Because much of the glacial deposits on

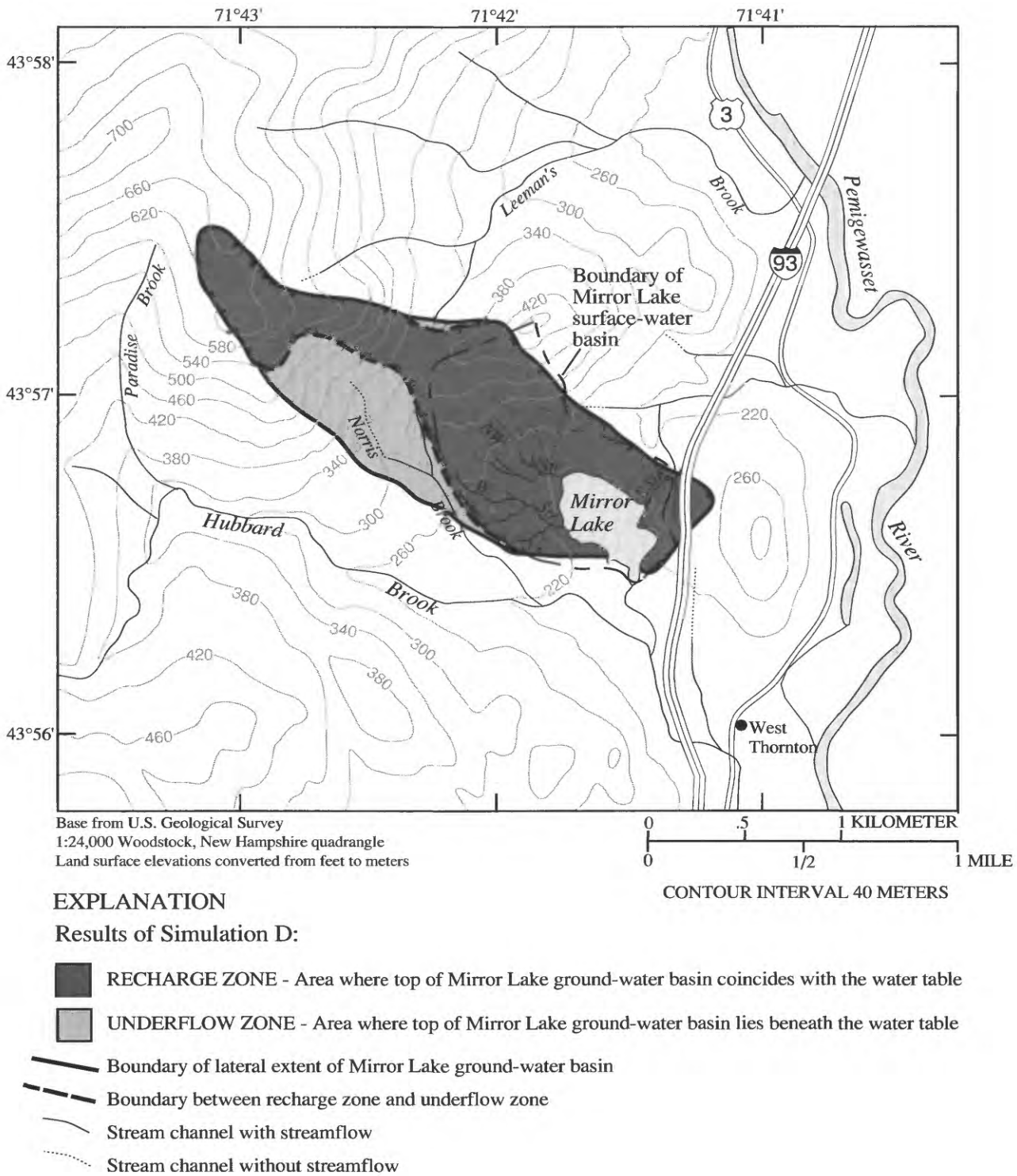

Figure 22. Horizontal extent of Mirror Lake ground-water basin in simulation D. Mirror Lake surface-water basin is included for comparison.

Table 10. Ground-water budget of Mirror Lake ground-water basin in simulations A and D.

[recharge, discharge, and flow in cubic meters per year; --, not computed]

Budget component	Value in simulation		Approximate, individual, 95% confidence interval[1]
	A	D	
Recharge to ground-water basin			
Precipitation to bedrock[2] (R_1)	172,000	147,000	161,000 to 183,000
Precipitation to glacial deposits[3] (R_2)	129,000	145,000	120,000 to 138,000
Streams to glacial deposits[4] (R_3)	6,000	5,000	5,000 to 7,000
Total Recharge ($R_T = R_1+R_2+R_3$)	307,000	297,000	--
Discharge from ground-water basin			
Glacial deposits to streams (D_1)	171,000	169,000	161,000 to 181,000
Glacial deposits to Mirror Lake (D_2)	133,000	125,000	126,000 to 140,000
Lacustrine mud sediments to Mirror Lake (D_3)	1,000	1,000	--
Bedrock to Mirror Lake[5] (D_4)	2,000	2,000	--
Total Discharge ($D_T = D_1+D_2+D_3+D_4$)	307,000	297,000	--
Flow between hydrogeologic units in ground-water basin			
Glacial deposits to bedrock (B_1)	18,000	34,000	13,000 to 23,000
Bedrock to glacial deposits (B_2)	187,000	178,000	174,000 to 200,000
Bedrock to gyttja (B_3)	1,000	1,000	--

[1]for simulation A only.
[2]in areas where simulated water table lies in bedrock.
[3]in areas where simulated water table lies in glacial deposits.
[4]along losing reaches of Streams W and NW.
[5]where bedrock crops out at east side of Mirror Lake.

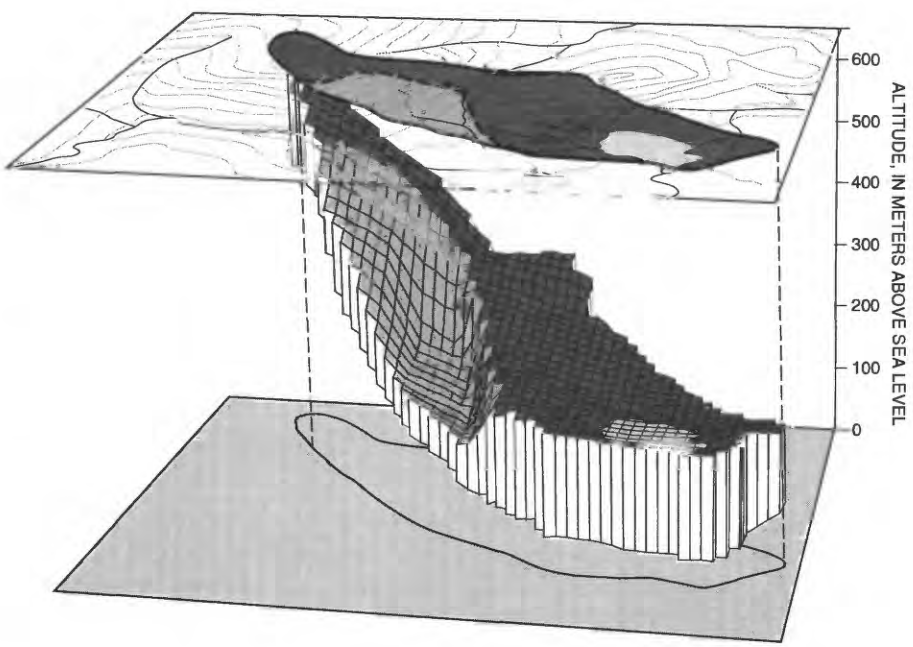

Figure 23. Three-dimensional extent of Mirror Lake ground-water basin in simulation D. See figure 22 for explanation.

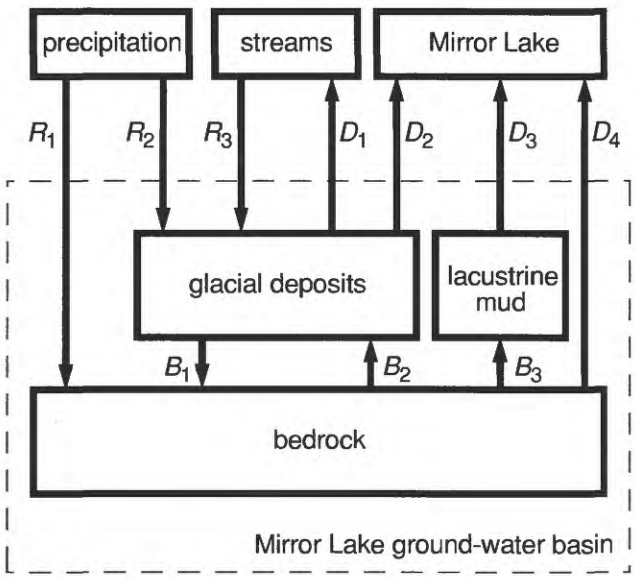

Figure 24. Components of ground-water budget for the Mirror Lake ground-water basin.

the upper hillsides are unsaturated, flow from glacial deposits to bedrock is relatively small. By contrast, flow from bedrock to glacial deposits (B_2) occurs primarily beneath lower hillsides and valleys, where the vertical flow component is predominantly upward. Flow from bedrock to the lacustrine mud or to the outcrop on the east side of Mirror Lake is minimal. Instead, nearly all flow from the bedrock is into the overlying glacial deposits. Therefore, flow from bedrock to glacial deposits is relatively large.

Uncertainties in the budget components given in table 10 can be assessed by calculating the approximate, individual, confidence interval for the components. The i^{th} budget component is denoted by y_i, and all budget components are contained in the vector $\hat{\boldsymbol{y}}$. To calculate the confidence intervals, it is first necessary to calculate the variance-covariance matrix for the budget components, which is (Hill, 1994, p. 28, eq. 12)

$$\boldsymbol{V}(\hat{\boldsymbol{y}}) = \chi \boldsymbol{V}(\hat{\boldsymbol{b}}) \chi^T \qquad (13)$$

where $\boldsymbol{V}(\hat{\boldsymbol{b}})$ is the variance-covariance matrix for the model parameters (see equation 5), and χ is a matrix containing derivatives of budget components, $\hat{\boldsymbol{y}}$, with respect to model parameters, $\boldsymbol{b}$, evaluated at the optimal parameters $\hat{\boldsymbol{b}}$. These derivatives are numerically calculated using a central-difference scheme. The square root of the i^{th} element on the main diagonal of $\boldsymbol{V}(\hat{\boldsymbol{y}})$ is the standard deviation, s_{y_i}, for the i^{th} budget component. The approximate, individual, 100(1-α) percent confidence interval for the i^{th} budget component is given by (Hill, 1994, p. 28, eq. 11)

$$\hat{y}_i \pm s_{y_i} \times t\left(n-p, 1-\frac{\alpha}{2}\right). \qquad (14)$$

where $t(n-p,1-a/2)$ is the 100(1-a/2) percentage point of the Student-t distribution with $n-p$ degrees of freedom.

Approximate, individual, 95-percent confidence intervals for budget components in simulation A are shown in table 10. These confidence intervals are relatively narrow, suggesting that the simulated budget components are relatively well constrained. However, caveats on confidence intervals for model parameters apply equally to confidence intervals for budget components. Because flow from lacustrine mud to Mirror Lake (D_3) and flow from bedrock to Mirror Lake (D_4) are both minute, their confidence intervals are not calculated because they are probably not meaningful. Confidence intervals for budget components in simulation D have similar widths as the corresponding ones in simulation A.

FLOW PATHS THROUGH THE GROUND-WATER BASIN

Of the total recharge to the Mirror Lake ground-water basin, a portion travels through the basin along flow paths that remain in glacial deposits, while the remainder travels along flow paths that involve movement in bedrock. These two types of flow paths are illustrated in figure 25. For simplicity, all ground water is shown to discharge into Mirror Lake; flow to the inlet streams is not illustrated. The stippled zone shows flow paths that remain in glacial deposits. Outside the stippled zone, flow paths involve movement in bedrock. The distinction between the two types of flow paths might be of importance to the chemical budget for Mirror Lake, because ground water that flows exclusively in glacial deposits might contain different amounts of dissolved chemicals than ground water that contacts bedrock. Note, however, that the travel distance in bedrock varies from relatively short (for example, flow path P-P') to relatively long (for example, flow path Q-Q').

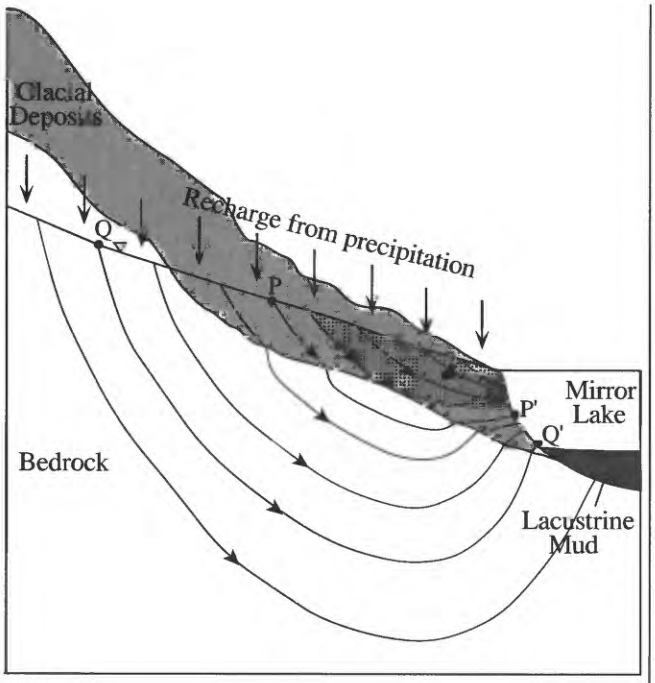

Figure 25. Flow paths through the Mirror Lake ground-water basin.

According to figure 24, the amount of ground-water flow that involves movement in bedrock is simply the total inflow to bedrock ($R_1 + B_1$), which also equals total outflow from bedrock ($B_2 + B_3 + D_4$). Calculations using budget components in table 10 indicate that 181,000 m^3/year (simulation D) to 190,000 m^3/year (simulation A) of ground-water flow involves movement in bedrock. This range is approximately 60 percent of total recharge to the ground-water basin. The amount of ground-water flow that remains in glacial deposits is the total recharge minus flow that involves movement in bedrock (that is, $R_T - R_1 - B_1$). Calculations using budget components in table 10 indicate 116,000 m^3/year (simulation D) to 117,000 m^3/year (simulation A) of ground-water flow travels exclusively in glacial deposits. This range is approximately 40 percent of total recharge to the ground-water basin.

These calculations indicate that simulations A and D yield similar amounts of ground-water flow that involves movement in the bedrock and that remains exclusively in the glacial deposits. Simulation D is expected to be the more realistic of the two simulations because calibration D matches the new hydraulic head observation at FS7 in the upper altitudes of the Mirror Lake area more closely than calibration A. However, the significant difference in water-table configuration between the two simulations at upper altitudes has a small effect on the calculated amount of ground-water flow through the bedrock and the glacial deposits over the Mirror Lake ground-water drainage basin.

SUMMARY

The Mirror Lake area discussed herein covers a 10-km^2 region in the eastern part of the Hubbard Brook valley in central New Hampshire. This area includes Mirror Lake, the three streams that flow into the lake, Leeman's Brook, Paradise Brook, and parts of Hubbard Brook and the Pemigewasset River. The topography of this area is characterized by steep hillsides and relatively flat valleys. Major hydrogeologic units include glacial deposits composed of till containing pockets of sand and gravel, and fractured crystalline bedrock composed of schist intruded by granite, pegmatite, and lamprophyre. A layer of lacustrine mud sediments covers much of the bottom of Mirror Lake.

Ground-water flow in the Mirror Lake area is typical of mountain-and-valley terrain of New England uplands. On hillsides, water from precipitation and snowmelt infiltrates to the water table, flows downslope through the saturated glacial deposits and fractured bedrock, and discharges to streams and to Mirror Lake. The water table generally is within 20 m of land surface, and in many locations, less than 10 m below land surface. At a well drilled on a ridge near the highest point of the study area, the water table is about 15 m below land surface. The shallow water table on the ridge suggests that the water table lies close to land surface over the entire Mirror Lake area.

A computer model was developed to simulate the three-dimensional, steady-state (long-term average) flow of ground water in the Mirror Lake area. A streamflow routing package was included in the model to simulate baseflow in streams and interaction between streams and ground water. The model assumes that recharge from precipitation is areally uniform, riparian evapotranspiration along stream banks can be neglected, flow in the bedrock occurs primarily in the uppermost 150 m, and distribution of hydraulic conductivity can be represented by dividing the flow domain into several zones, each having

uniform properties. Because local variations in recharge and hydraulic conductivities are ignored, the simulation results characterize the generalized ground-water flow system, not local details.

The model was calibrated using nonlinear least-squares regression to match long-term average hydraulic heads measured in piezometers and bedrock wells, and long-term average baseflow in the three inlet streams to Mirror Lake. Long-term average baseflow was assumed to be 40 percent of long-term average streamflow as measured in flumes. Model calibration yielded 26 to 28 cm/year of recharge from precipitation to the water table, and hydraulic conductivities of 1.7×10^{-6} to 2.7×10^{-6} m/s for glacial deposits, about 3×10^{-7} m/s for bedrock beneath lower hillsides and valleys, and about 6×10^{-8} m/s for bedrock beneath upper hillsides and hilltops. Analysis of parameter uncertainty indicates that the above values are well constrained, at least within the context of regression analysis. In the regression, several attributes of the ground-water flow model are assumed perfectly known. The value of hydraulic conductivity for bedrock beneath upper hillsides and hilltops was determined from few data, and additional hydraulic-head observations are required to confirm this result. Model fit was not improved by introducing a 10-to-1 ratio of horizontal-to-vertical anisotropy in hydraulic conductivity of glacial deposits, or by varying hydraulic conductivity with depth in the modeled part (uppermost 150 m) of the bedrock.

Model simulation indicates that, in significant parts of the model domain, the water table lies in bedrock. Outside these areas, the water table lies in glacial deposits. Where the water table lies in bedrock, glacial deposits are either unsaturated or absent; recharge from precipitation enters the bedrock either by infiltration through the overlying unsaturated glacial deposits, or directly from land surface where bedrock crops out. Unsaturated glacial deposits are mostly on upper hillsides and away from streams.

The calibrated model was used to delineate the Mirror Lake ground-water basin, which is defined as the volume of subsurface through which ground water flows from the water table to Mirror Lake or its inlet streams. Results indicate that Mirror Lake and its inlet streams drain an area of ground-water recharge that is about 1.5 times the area of the surface-water basin. The ground-water basin extends far up the hillside on the northwestern part of the study area. Ground water from this area flows at depth beneath Norris Brook and discharges into Mirror Lake or its inlet streams. As a result, the Mirror Lake ground-water basin extends beneath the adjacent ground-water basin that drains into Norris Brook.

Ground-water budget calculations indicate that approximately 300,000 m^3/year of precipitation recharges the Mirror Lake ground-water basin. About half the recharge enters the basin in areas where the simulated water table lies in glacial deposits; the other half enters the basin in areas where the simulated water table lies in bedrock. Flow from glacial deposits to bedrock occurs primarily under upper hillsides, where the vertical flow component is predominantly downward. Flow from bedrock to glacial deposits occurs primarily under lower hillsides and valleys, where the vertical flow component is predominantly upward. About 40 percent of recharge (120,000 m^3/year) travels through the basin along flow paths that remain exclusively in glacial deposits; about 60 percent (180,000 m^3/year) travels along flow paths that involve movement in bedrock. Under steady state, total recharge to the ground-water basin equals total discharge from the basin. Of the total discharge, slightly more than half (170,000 m^3/year) flows into the three Mirror Lake inlet streams; slightly less than half (130,000 m^3/year) flows directly into Mirror Lake.

REFERENCES CITED

Boelter, D.H., 1972, Methods for analysing the hydrological characteristics of organic soils in marsh-ridden areas, *in* Hydrology of marsh-ridden areas, Proceedings of the Minsk Symposium, June, 1972: Paris, The Unesco Press, p. 161–169.

Bouwer, H., and Rice, R.C., 1976, A slug test for determining hydraulic conductivity of unconfined aquifers with completely or partially penetrating wells: Water Resources Research, v. 12, no. 3, p. 423–428.

Cooley, R.L., and Naff, R.L., 1990, Regression modeling of ground-water flow: U.S. Geological Survey Techniques of Water-Resources Investigations, Book 3, Chapter B4, 232 p.

Cooper, H.H., Jr., Bredehoeft, J.D., and Papadopulos, I.S., 1967, Response of a finite-diameter well to an instantaneous charge of water: Water Resources Research, v. 3, no. 1, p. 263–269.

Davis, M.B., and Ford, M.S.J., 1982, Sediment focusing in Mirror Lake, New Hampshire: Limnology and Oceanography, v. 27, no. 1, p. 137–150.

Demir, Zafer, 1992, Some contributions to Hvorslev tests, slug tests, and drill-stem tests: Berkeley, University of California, M.S. thesis, 107 p.

Federer, C.A., Flynn, L.D., Martin, C.W., Hornbeck, J.W., and Pierce, R.S., 1990, Thirty years of hydrometeorologic data at the Hubbard Brook Experimental Forest, New Hampshire: U.S. Department of Agriculture, Forest Service, Northeastern Forest Experiment Station, General Technical Report NE-141, 44 p.

Frape S.K., and Patterson, R.J., 1981, Chemistry of interstitial water and bottom sediments as indicators of seepage patterns in Perch Lake, Chalk River, Ontario: Limnology and Oceanography, v. 26, p. 500–517.

Freeze, R.A., and Cherry, J.A., 1979, Groundwater: Englewood Cliffs, N.J., Prentice-Hall, 604 p.

Haeni, F.P., Lane, J.W., Jr., and Lieblich, D.A., 1993, Use of surface-geophysical and borehole-radar methods to detect fractures in crystalline rocks, Mirror Lake area, Grafton County, New Hampshire, *in* Banks, Sheila, and Banks, David, eds., IAH memoires of the 24th congress, hydrogeology of hard rocks, As, Norway, June 28 to July 2, 1993: International Association of Hydrogeologists, p. 577–587.

Harbaugh, A.W., 1990, A computer program for calculating subregional water budgets using results from the U.S. Geological Survey modular three-dimensional finite-difference ground-water flow model: U.S. Geological Survey Open-File Report 90-392, 46 p.

Hardin, E.L., Cheng, C.H., Paillet, F.L., and Mendelson, J.D., 1987, Fracture characterization by means of attenuation and generation of tube waves in fractured crystalline rock at Mirror Lake, New Hampshire: Journal of Geophysical Research, v. 92, no. B8, p. 7989–8006.

Harte, P.A., 1992, Regional ground-water flow in crystalline bedrock and interaction with glacial drift in the New England uplands: Durham, University of New Hampshire, M.S. thesis, 141 p.

Harte, P.A., 1994, Comparison of vertical discretization techniques in finite-difference models of ground-water flow: Example from a hypothetical New England setting: U.S. Geological Survey Open-File Report 94-343, 25 p.

Hill, M.C., 1990, Preconditioned conjugate-gradient 2 (PCG2), a computer program for solving ground-water flow equations: U.S. Geological Survey Water-Resources Investigations Report 90-4048, 43 p.

Hill, M.C., 1992, A computer program (MODFLOWP) for estimating parameters of a transient, three-dimensional, ground-water flow model using nonlinear regression: U.S. Geological Survey Open-File Report 91-484, 358 p.

Hill, M.C., 1994, Five computer programs for testing weighted residuals and calculating linear confidence and prediction intervals on results from the ground-water parameter-estimation computer program MODFLOWP: U.S. Geological Survey Open-File Report 93-481, 81 p.

Hsieh, P.A., Perkins, R.L., and Rosenberry, D.O., 1996, Field instrumentation for multilevel monitoring of hydraulic head in fractured bedrock at the Mirror Lake site, Grafton County, New Hampshire, *in* Morganwalp, D.W., and Aronson, D.A., eds., U.S. Geological Survey Toxic Substances Hydrology Program—Proceedings of the Technical Meeting, Colorado Springs, Colorado, September 20–24, 1993: U.S. Geological Survey Water-Resources Investigations Report 94-4015, v. 1, p. 137–140.

Hsieh, P.A., and Shapiro, A.M., 1994, Analyzing cross-hole hydraulic tests in fractured crystalline rock: An example from the Mirror Lake site, New Hampshire [abs.]: Eos, Transactions, American Geophysical Union, v. 75, no. 16, supplement, 1994 Spring Meeting, p. 153.

Hsieh, P.A., Shapiro, A.M., Barton, C.C., Haeni, F.P., Johnson, C.D., Martin, C.W., Paillet, F.L., Winter, T.C., and Wright, D.L., 1993, Methods of characterizing fluid movement and chemical transport in fractured rocks, *in* Cheney, J.T., and Hepburn, J.C., eds., Field trip guidebook for the northeastern United States: 1993 Boston GSA: Amherst, University of Massachusetts, Department of Geology and Geography, Contribution No. 67, p. R1-R30.

Institute of Hydrology, 1980a, Low flow studies: Wallingford, United Kingdom, Institute of Hydrology Report, no. 1.

Institute of Hydrology, 1980b, Low flow studies: Wallingford, United Kingdom, Institute of Hydrology Report, no. 3.

Lane, J.W., Jr., Haeni, F.P., and Watson, W.M., 1995, Use of a square-array direct-current resistivity method to detect fractures in crystalline bedrock in New Hampshire: Ground Water, v. 33, no. 3, p. 476–485.

Likens, G.E., Bormann, F.H., Pierce, R.S., Eaton, J.S., and Johnson, N.M., 1977, Biogeochemistry of a forested ecosystem: New York, Springer-Verlag, 146 p.

Likens, G.E., ed., 1985, An ecosystem approach to aquatic ecology, Mirror Lake and its environment: New York, Springer-Verlag, 516 p.

Likens, P.C., 1991, Publications of the Hubbard Brook Ecosystem Study: Millbrook, N.Y., Institute of Ecosystem Studies, 109 p.

Lyons, J.B., Bothner, W.A., Moench, R.H., and Thompson, J.B., Jr., eds., 1986, Interim geologic map of New Hampshire: Concord, New Hampshire Department of Resources and Economic Development, Open-File Report 86-1, 1 sheet, scale 1:250,000.

Mau, D.P., and Winter, T.C., 1997, Estimating ground-water recharge from streamflow hydrographs for a small watershed in a temperate humid climate, New Hampshire, USA: Ground Water, v. 35 [in press].

McDonald, M.G., and Harbaugh, A.W., 1988, A modular three-dimensional finite-difference ground-water flow model: U.S. Geological Survey Techniques of Water-Resources Investigations, Book 6, Chapter A1, 586 p.

McHone, J.G., 1984, Mesozoic igneous rocks of northern New England and adjacent Quebec: Summary, description map, and bibliography of data sources: Geological Society of America, Map and Chart Series, MC-49.

Moeller, R.E., 1978, The hydrophytes of Mirror Lake: A study of vegetational structure and seasonal biomass dynamics: Ithica, N.Y., Cornell University, Ph.D. dissertation, 212 p.

Morganwalp, D.W., and Aronson, D.A., eds., 1996, U.S. Geological Survey Toxic Substances Hydrology Program—Proceedings of the Technical Meeting, Colorado Springs, Colorado, September 20–24, 1993: U.S. Geological Survey Water-Resources Investigations Report 94-4015, 1113 p.

Paillet, F.L., 1985, Geophysical well log data for study of water flow in fractures in bedrock near Mirror lake, West Thornton, New Hampshire: U.S. Geological Survey Open-File Report 85-340, 27p.

Paillet, F.L., Hess, A.E., Cheng, C.H., and Hardin, E.L., 1987, Characterization of fracture permeability with high-resolution vertical flow measurements during borehole pumping: Ground Water, v. 25, no. 1, p. 28–40.

Paillet, F.L., and Kapucu, K., 1989, Fracture characterization and fracture-permeability estimates from geophysical logs in the Mirror Lake watershed, New Hampshire: U.S. Geological Survey Water-Resources Investigations Report 89-4058, 49 p.

Pollack, D.W., 1994, User's guide for MODPATH/MODPATH-PLOT, version 3: A particle tracking post-processing package for MODFLOW, the U.S. Geological Survey finite-difference ground-water flow model: U.S. Geological Survey Open-File Report 94-0464, 249 p.

Prudic, D.E., 1989, Documentation of a computer program to simulate stream-aquifer relations using a modular, finite-difference, ground-water flow model: U.S. Geological Survey Open-File Report 88-729, 113 p.

Rosenberry, D.O., and Winter, T.C., 1993, The significance of fracture flow to the water balance of a lake situated in fractured crystalline rock terrane, *in* Banks, Sheila, and Banks, David, eds., IAH Memoires of the 24th Congress, Hydrogeology of Hard Rocks, As, Norway, June 28 to July 2, 1993: International Association of Hydrogeologists, p. 967–977.

Rutledge, A.T., 1993, Computer programs for describing the recession of ground-water discharge and for estimating mean ground-water recharge and discharge from streamflow records: U.S. Geological Survey Water-Resources Investigations Report 93-4121, 45 p.

Rutledge, A.T., and Daniel, C.C., III, 1994, Testing an automated method to estimate ground-water recharge from streamflow records: Ground Water, v. 32, no. 2, p. 180–189.

Shapiro, A.M., and Hsieh, P.A., 1991, Research in fractured-rock hydrogeology: Characterizing fluid movement and chemical transport in fractured rock at the Mirror Lake drainage basin, New Hampshire, *in* Mallard, G.E., and Aronson, D.A., eds., U.S. Geological Survey Toxic Substances Hydrology Program—Proceedings of the technical meeting, Monterey, California, March 11–15, 1991: U.S. Geological Survey Water-Resources Investigations Report 91-4034, p. 155–161.

Shattuck, P.C., 1991, Shallow water-table response to precipitation and evapotranspiration in an ephemeral stream valley, Woodstock, New Hampshire: Durham, University of New Hampshire, M.S. thesis, 113 p.

U.S. Department of Agriculture Forest Service, 1991, The Hubbard Brook Ecosystem Study: Site Description and Research Activities: Northeastern Forest Experimental Station NE-INF-96-91, 61 p.

Wilson, Alicia, 1991, Distribution of hydraulic conductivity in the glacial drift at Hubbard Brook Experimental Forest, West Thornton, New Hampshire: Hanover, N.H., Dartmouth College, Department of Earth Sciences, Senior honors thesis, 56 p.

Winter, T.C., 1984, Geohydrologic setting of Mirror Lake, West Thornton, New Hampshire: U.S. Geological Survey Water-Resources Investigations Report 84-4266, 61 p.

Winter, T.C., 1985, Physiographic setting and geologic origin of Mirror Lake, *in* Likens, G.E., ed., An ecosystem approach to aquatic ecology, Mirror Lake and Its Environment: New York, Springer-Verlag, p. 40–53.

Winter, T.C., Eaton, J.S., and Likens, G.E., 1989, Evaluation of inflow to Mirror Lake, New Hampshire: Water Resources Bulletin, v. 25, no. 5, p. 991–1008.